



Leibniz-Institut für
Astrophysik Potsdam

Photospheric and Chromospheric Observations of Dynamic Features in an Arch Filament System

S. J. González Manrique (smanrique@aip.de)

C. Kuckein, A. Pastor Yabar, M. Collados, C. Denker, M. Verma,
A. Diercke, H. Balthasar, P. Gömöry, M. Cubas Armas, A. Lagg,
S. Solanki, and K. Strassmeier

AIP, UP, IAC, ULL, KIS, AISAS, MPS, and SSR

Observations

- ❑ 8:16 UT on 17 April 2015
- ❑ Two small pores
- ❑ Coordinates:
 $x = 64''$ $y = -232''$
- ❑ $\mu = 0.97$
- ❑ Observed spectral lines:

CRISP:

Fe I 617.3 nm

Ca II 854.2 nm

GFPI:

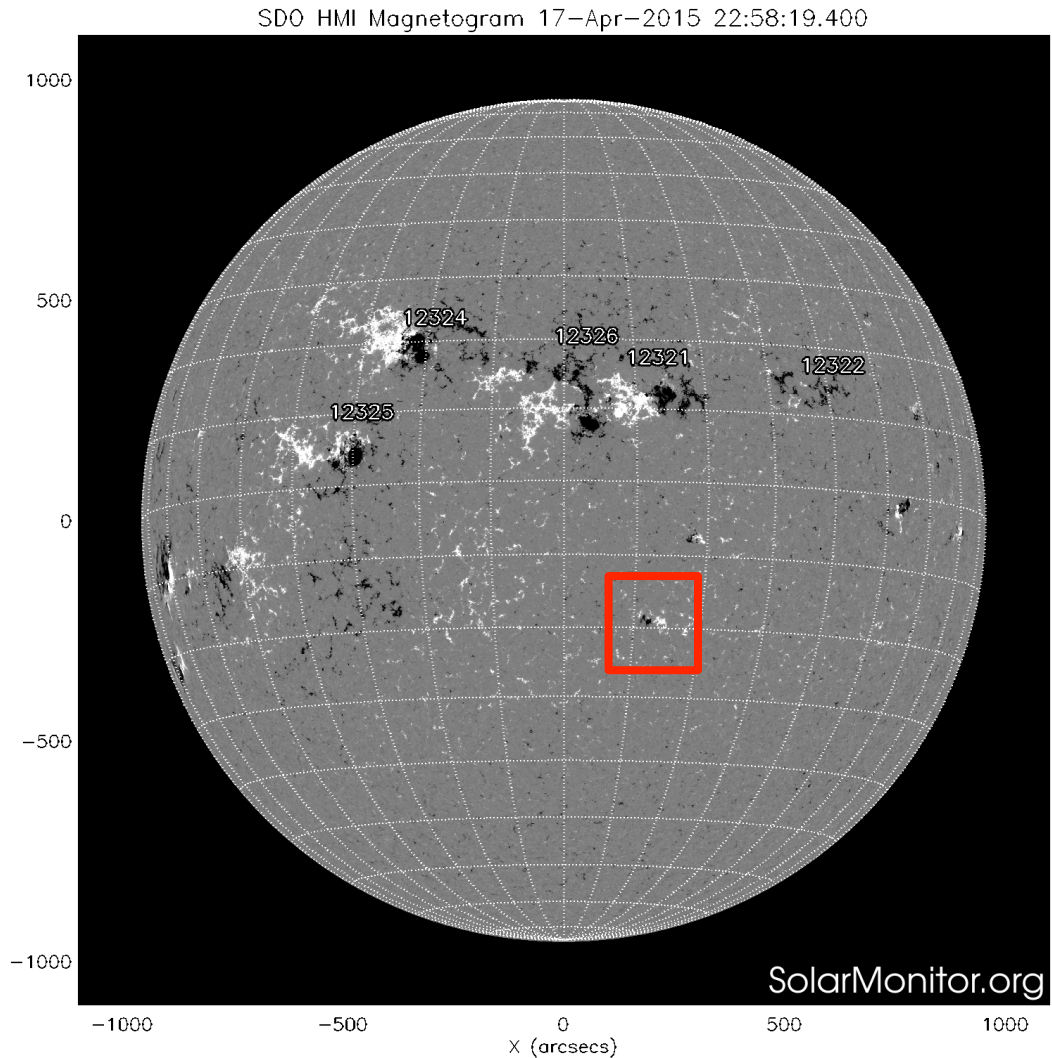
Fe I 630.2 nm

GRIS:

Si I 1082.7 nm

He I 1083.0 nm

Ca I 1083.9 nm



Observations

- ❑ 8:16 UT on 17 April 2015
- ❑ Two small pores
- ❑ Coordinates:
 $x = 64''$ $y = -232''$
- ❑ $\mu = 0.97$
- ❑ Observed spectral lines:

CRISP:

Fe I 617.3 nm

Ca II 854.2 nm

GFPI:

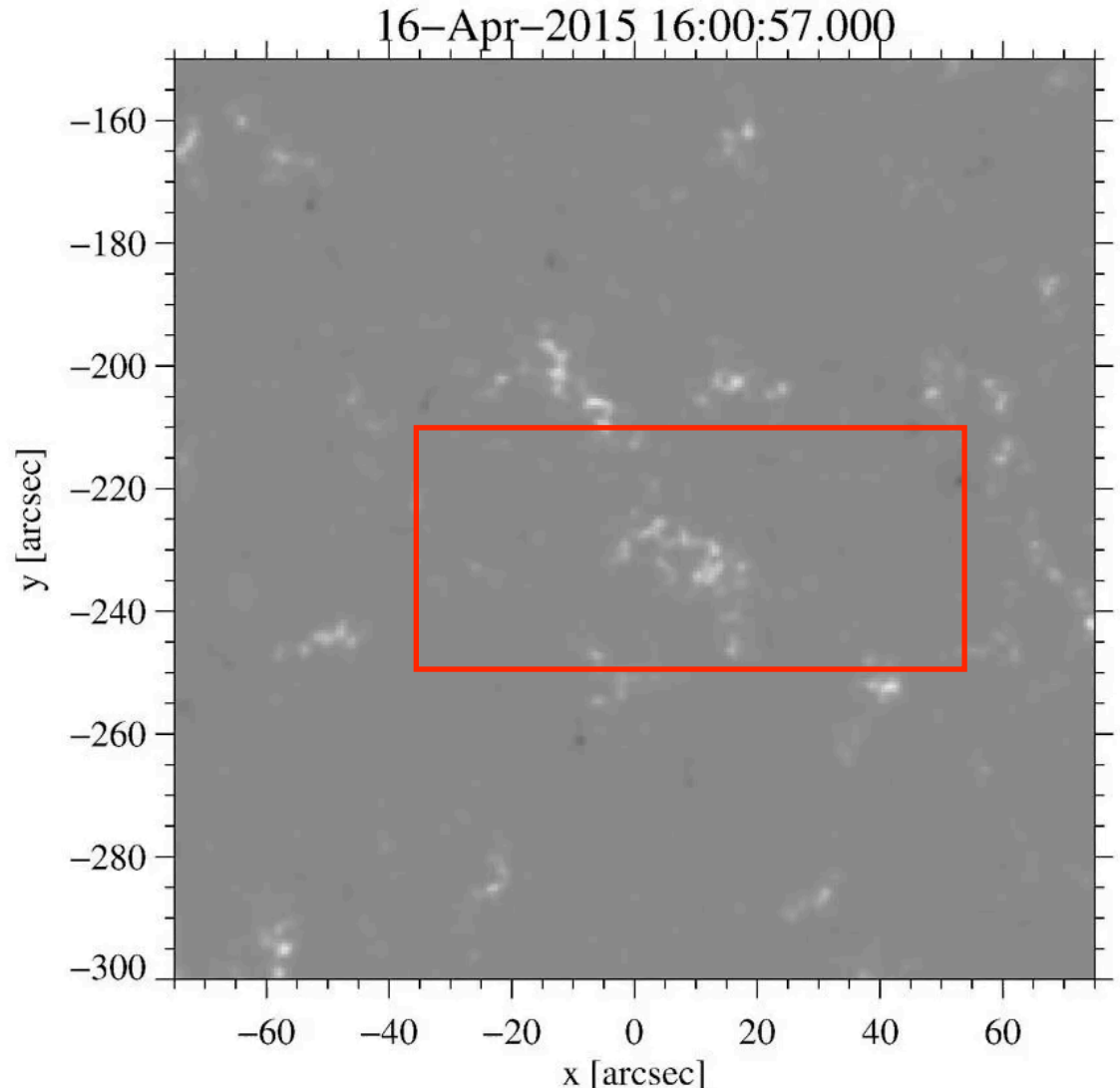
Fe I 630.2 nm

GRIS:

Si I 1082.7 nm

He I 1083.0 nm

Ca I 1083.9 nm



Line-of-sight magnetograms SDO/HMI

Observations

- ❑ 8:16 UT on 17 April 2015
- ❑ Two small pores
- ❑ Coordinates:
 $x = 64''$ $y = -232''$
- ❑ $\mu = 0.97$
- ❑ Observed spectral lines:

CRISP:

Fe I 617.3 nm

Ca II 854.2 nm

GFPI:

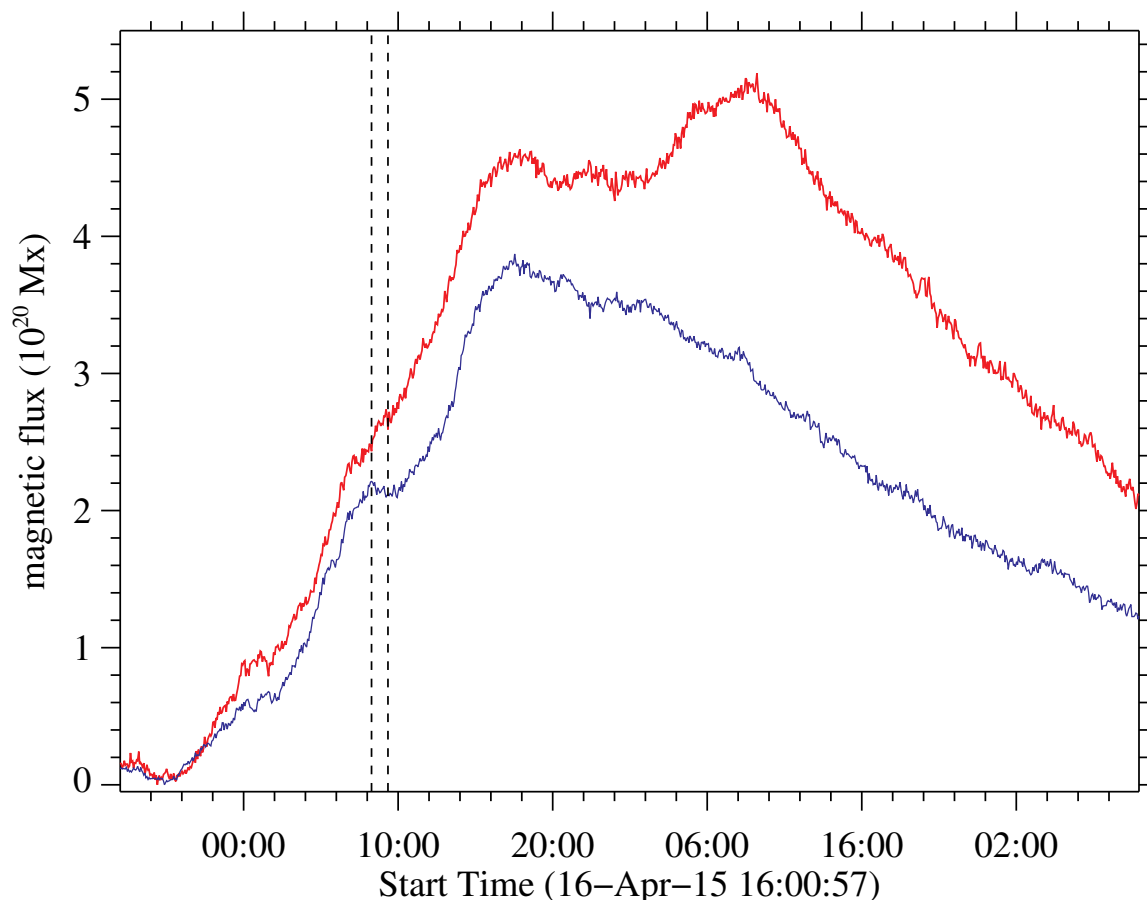
Fe I 630.2 nm

GRIS:

Si I 1082.7 nm

He I 1083.0 nm

Ca I 1083.9 nm



Observations

- ❑ 8:16 UT on 17 April 2015
- ❑ Two small pores
- ❑ Coordinates:
 $x = 64''$ $y = -232''$
- ❑ $\mu = 0.97$
- ❑ Observed spectral lines:

CRISP:

Fe I 617.3 nm

Ca II 854.2 nm

GFPI:

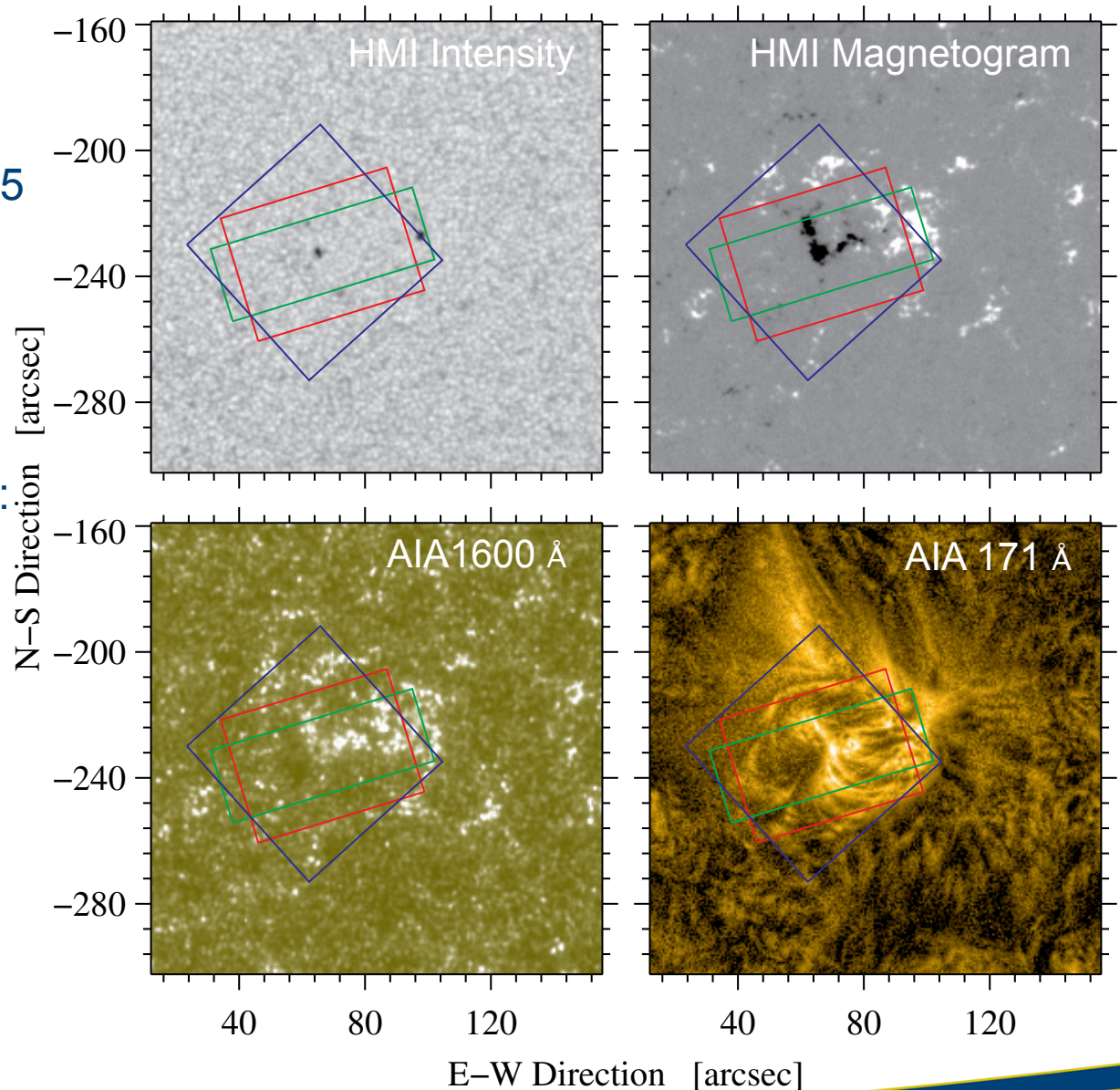
Fe I 630.2 nm

GRIS:

Si I 1082.7 nm

He I 1083.0 nm

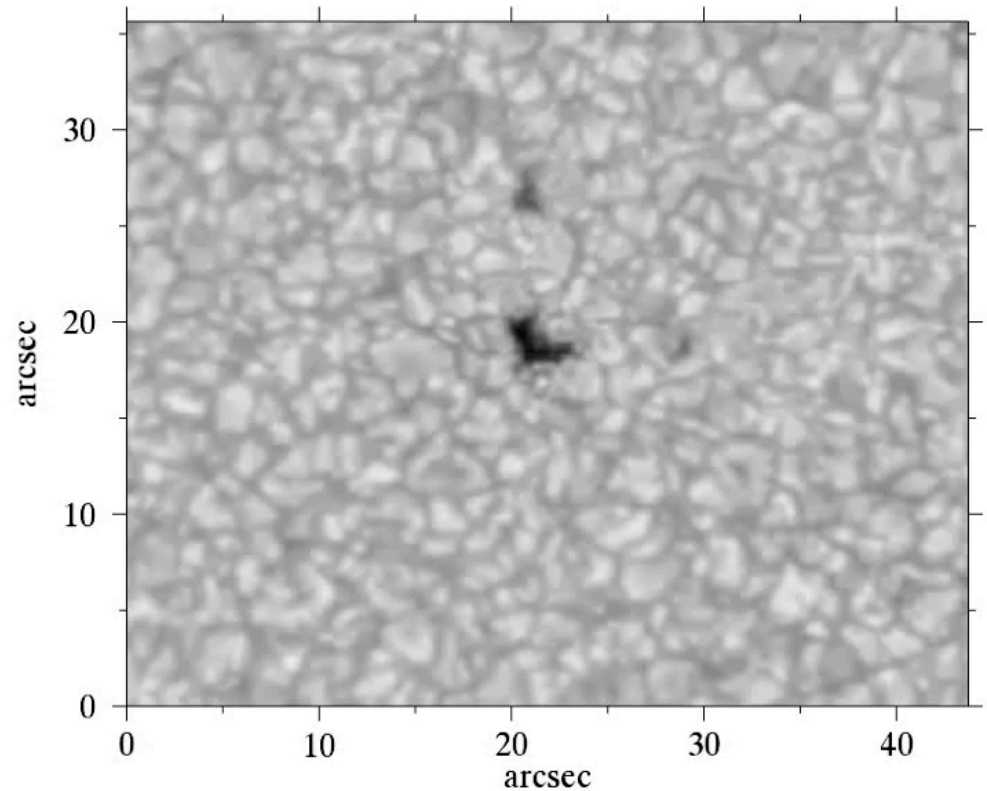
Ca I 1083.9 nm



Observations

GFPI:

- ❑ Start observations:
08:47 UT on 17 April 2015
- ❑ Broad-band images
- ❑ 2×2 binning
- ❑ Imaging spectroscopy:
 - ❑ Spectral line: Fe I 630.2 nm
 - ❑ Cadence: 53 s
 - ❑ Exposure time: 20 ms
 - ❑ Spectral steps: 54
 - ❑ Scans: 72
 - ❑ Accumulations: 8
- ❑ Data reduction with sTools (see poster Kuckein et al. and Kuckein et al. (2017), arXiv)

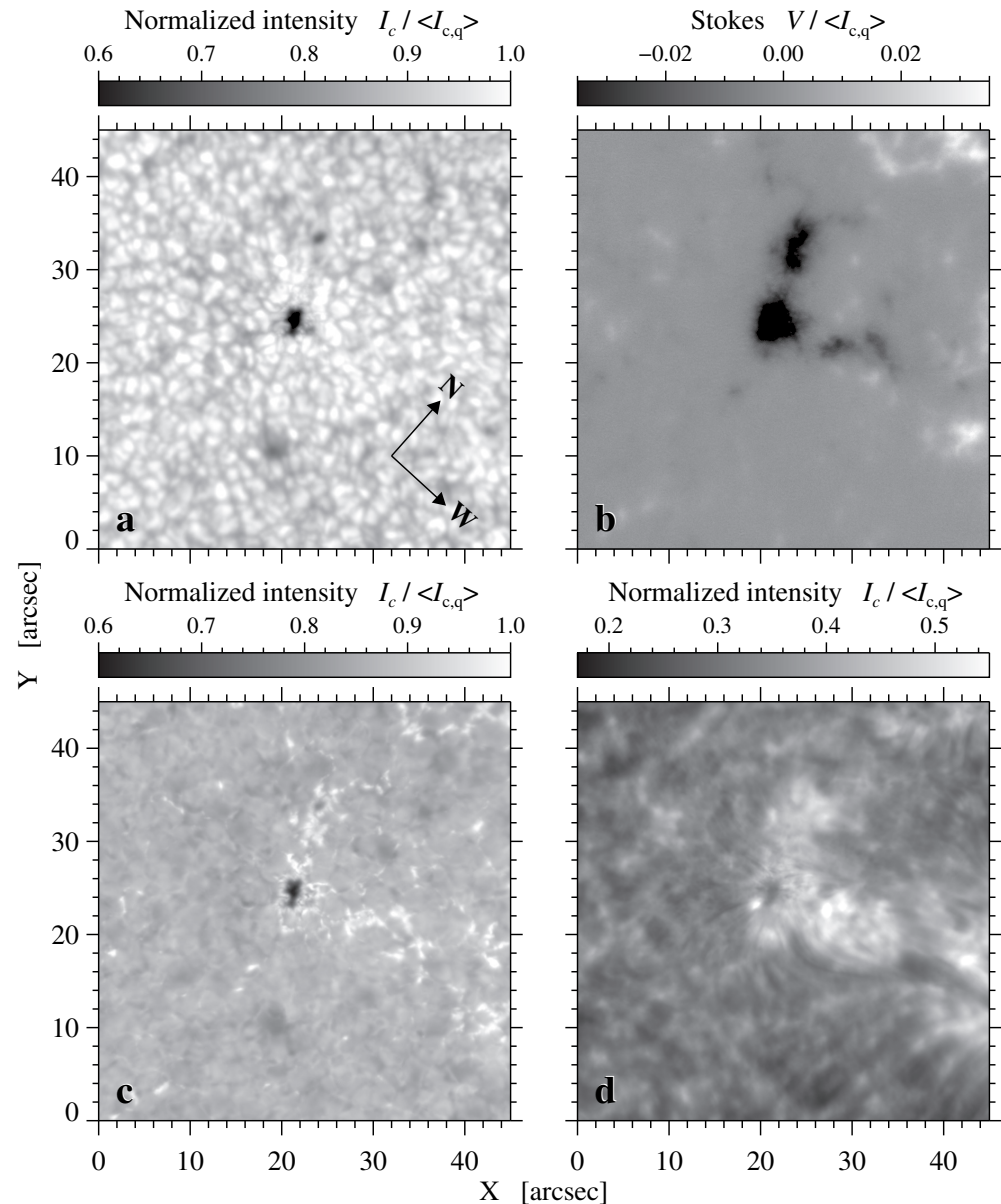


Restored (MOMFBD) broad-band images using the sTools data pipeline.

Observations

CRISP:

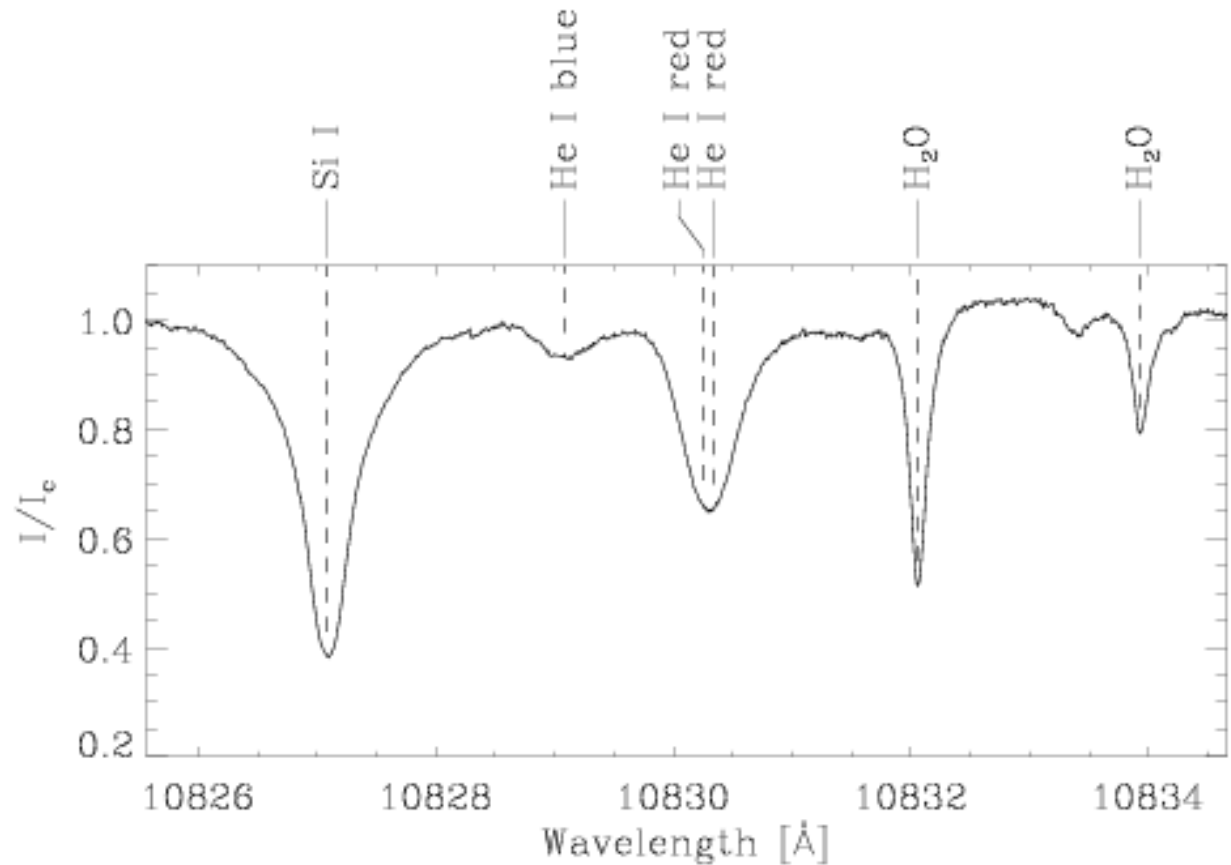
- Start observations: 08:47 UT on 17 April 2015
- Imaging spectropolarimetry:
 - Spectral lines: Fe I 617.3 nm
Ca II 854.2 nm
 - Cadence: 44 s
 - Spectral steps: 20 (Fe I)
 - Spectral steps: 21 (Ca II)
 - Scans: 50



Observations

GRIS:

- Start observations: 08:16 UT on 17 April 2015
- Very fast spectroscopic mode
- Spectral region: 1083.0 nm
- Photospheric Si I and chromospheric He I spectra among others
- Steps: 180
- Stepsize: 0.134"
- Pixel size: 0.137" along the slit
- Integration time: 100 ms
- 65 maps
- Cadence: 58 s



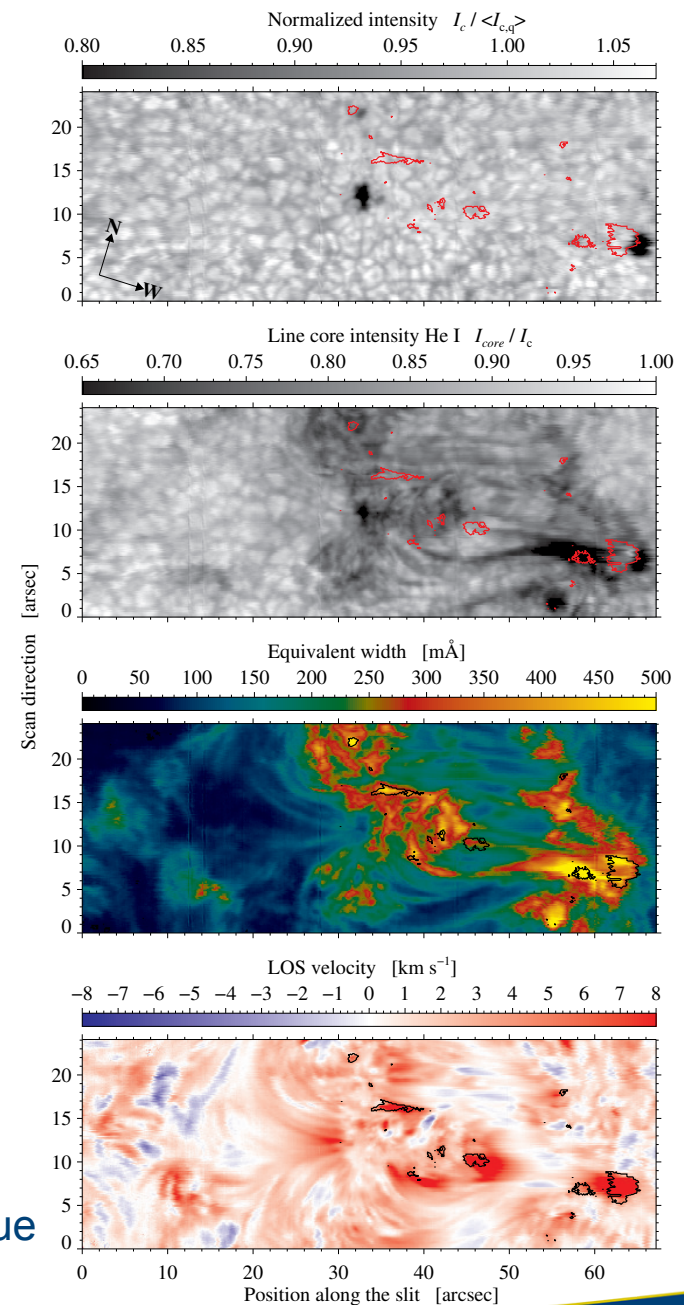
Kuckein et al. (2012b)

Observations

GRIS:

- ❑ Start observations:
08:16 UT on 17 April 2015
- ❑ Very fast spectroscopic mode
- ❑ Spectral region: 1083.0 nm
- ❑ Photospheric Si I and chromospheric He I spectra among others
- ❑ Steps: 180
- ❑ Stepsize: 0.134"
- ❑ Pixel size: 0.137" along the slit
- ❑ Integration time: 100 ms
- ❑ 65 maps
- ❑ Cadence: 58 s

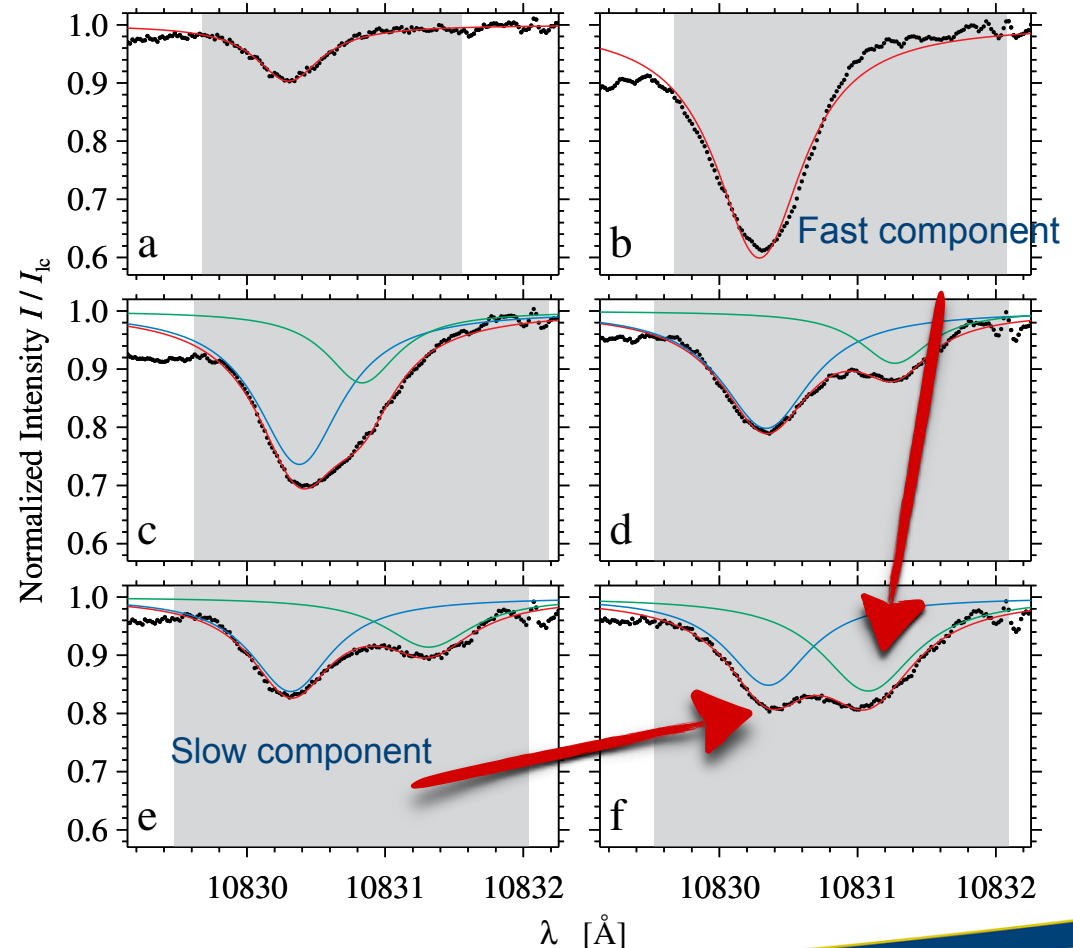
González Manrique
et al. (2016)



Fitting spectral profiles in He I 1083.0 nm

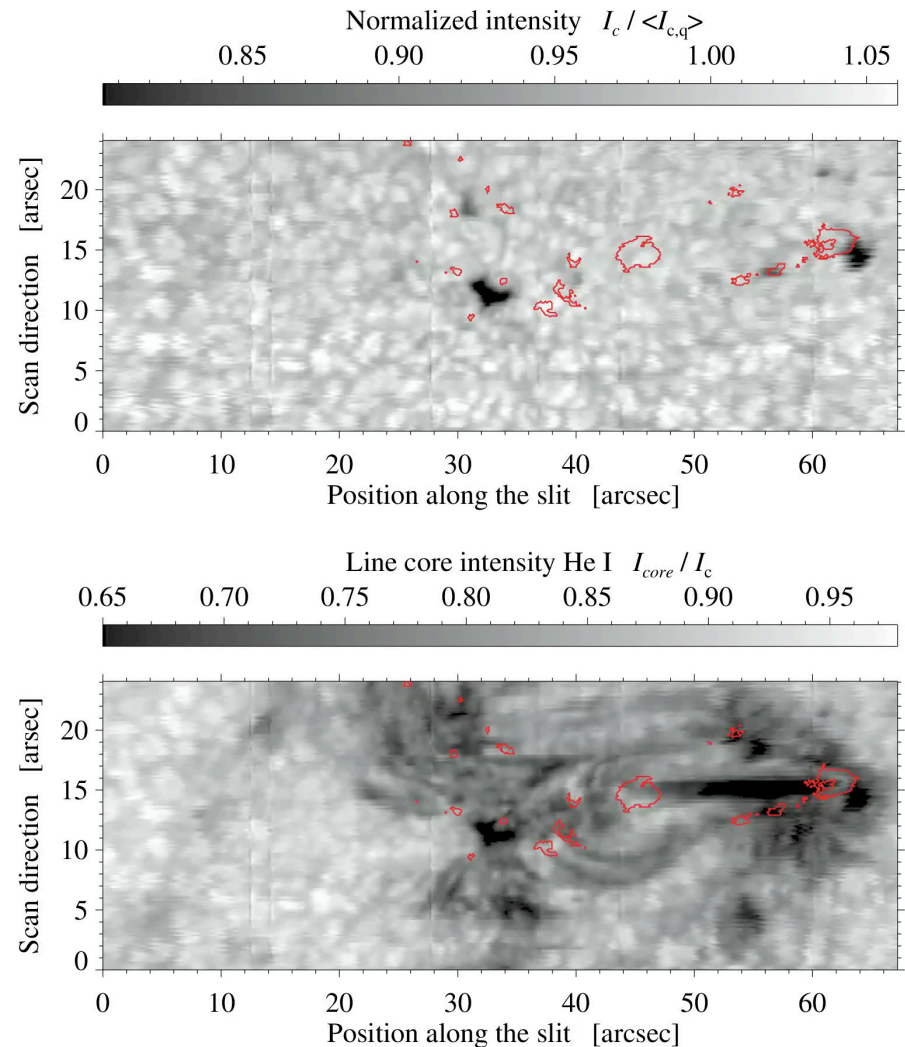
González Manrique et al. (2016)

- ❑ Two atmospheric components located within the same resolution element (Lagg et al., 2007)
- ❑ Two or more peaks next to the red component of He I (e.g., Sasso et al., 2011, 2007)
- ❑ Slow component often subsonic
- ❑ Fast component reaches supersonic velocities
- ❑ Dual-flow components reported in different phenomena. For example, flares (Teriaca et al., 2003), (Sasso et al., 2011, 2007), emerging flux process (Lagg et al., 2007), pores, etc.
- ❑ Typical velocity range 40 – 90 km/s



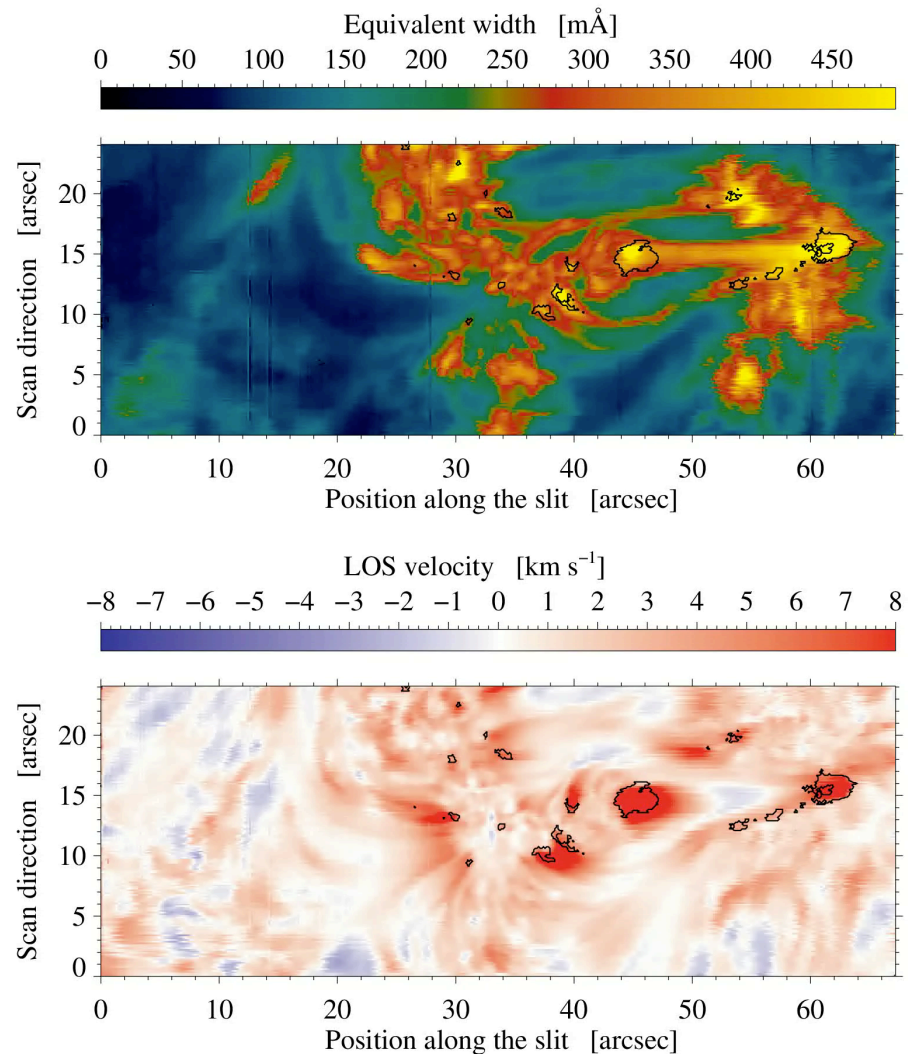
Temporal evolution of an arch filament system

- ❑ One-hour evolution of the EFR
- ❑ The He I line-core intensity maps show an AFS connecting two opposite polarities.
- ❑ Time-space diagrams are created at the position of the yellow line.
- ❑ Equivalent width is higher in the absorption features.
- ❑ The contours encompass only clearly discernible dual-flow components in the He I profiles.
- ❑ Single maps of Ca I and Si I line-core velocity do not show a clear connection from the chromosphere to the photosphere.



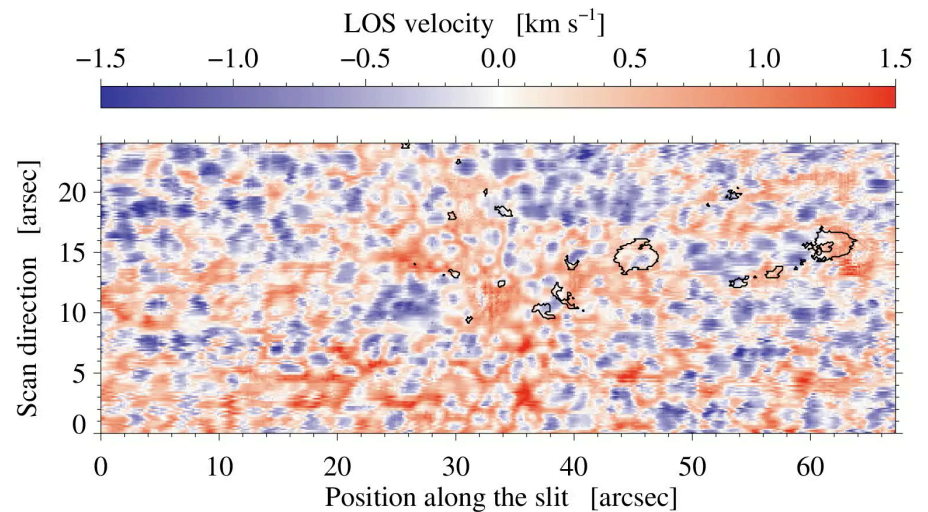
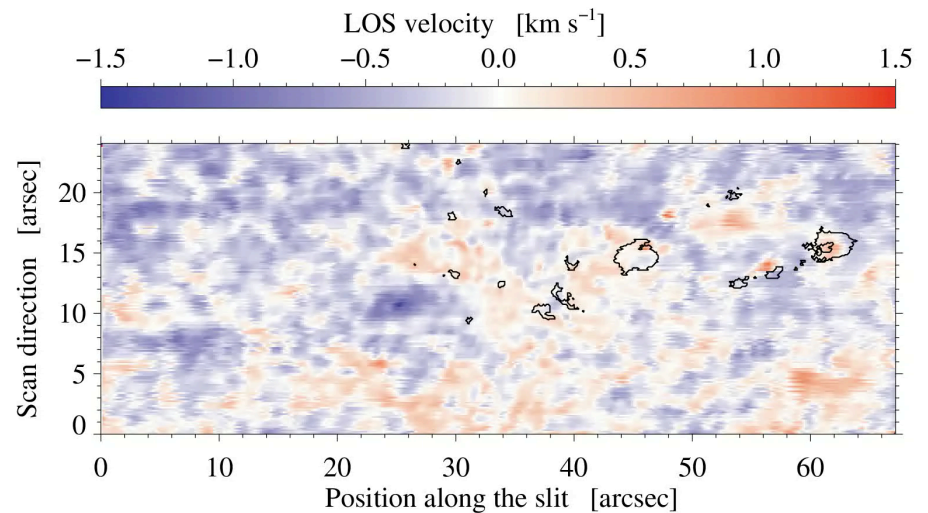
Temporal evolution of an arch filament system

- ❑ One-hour evolution of the EFR
- ❑ The He I line-core intensity maps show an AFS connecting two opposite polarities.
- ❑ Time-space diagrams are created at the position of the yellow line.
- ❑ Equivalent width is higher in the absorption features.
- ❑ The contours encompass only clearly discernible dual-flow components in the He I profiles.
- ❑ Single maps of Ca I and Si I line-core velocity do not show a clear connection from the chromosphere to the photosphere.



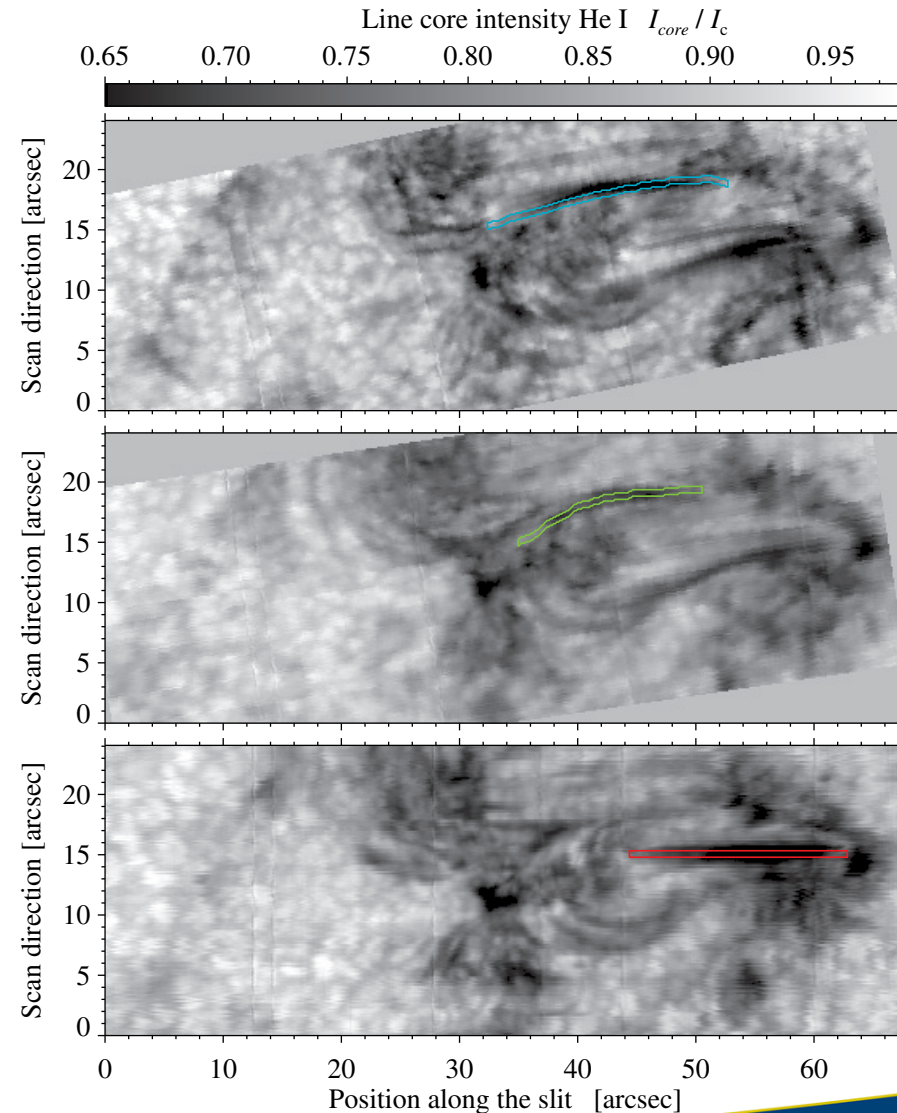
Temporal evolution of an arch filament system

- ❑ One-hour evolution of the EFR
- ❑ The He I line-core intensity maps show an AFS connecting two opposite polarities.
- ❑ Time-space diagrams are created at the position of the yellow line.
- ❑ Equivalent width is higher in the absorption features.
- ❑ The contours encompass only clearly discernible dual-flow components in the He I profiles.
- ❑ Single maps of Ca I and Si I line-core velocity do not show a clear connection from the chromosphere to the photosphere.

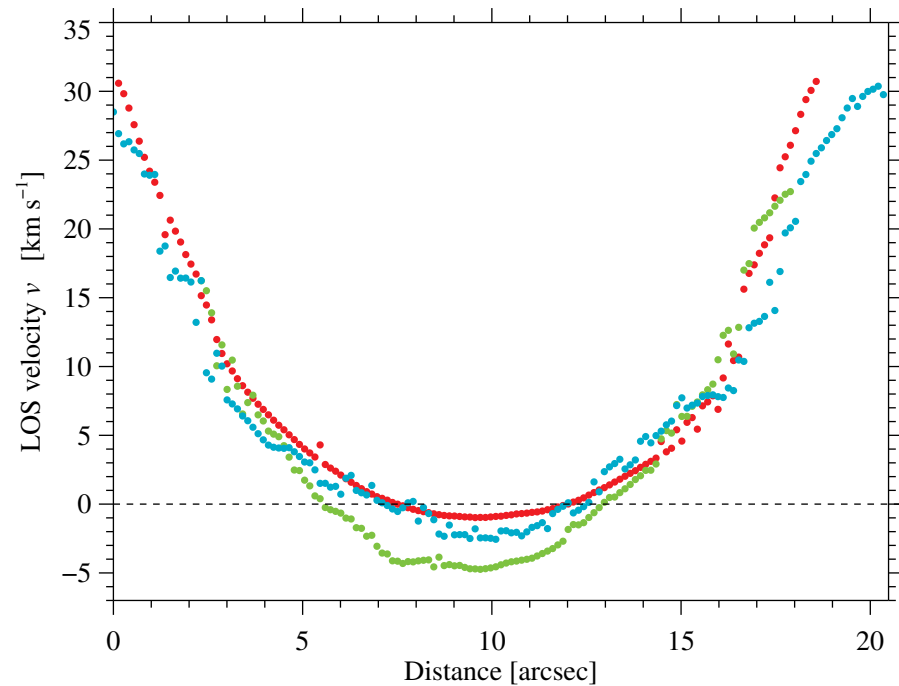


Temporal evolution of an arch filament system

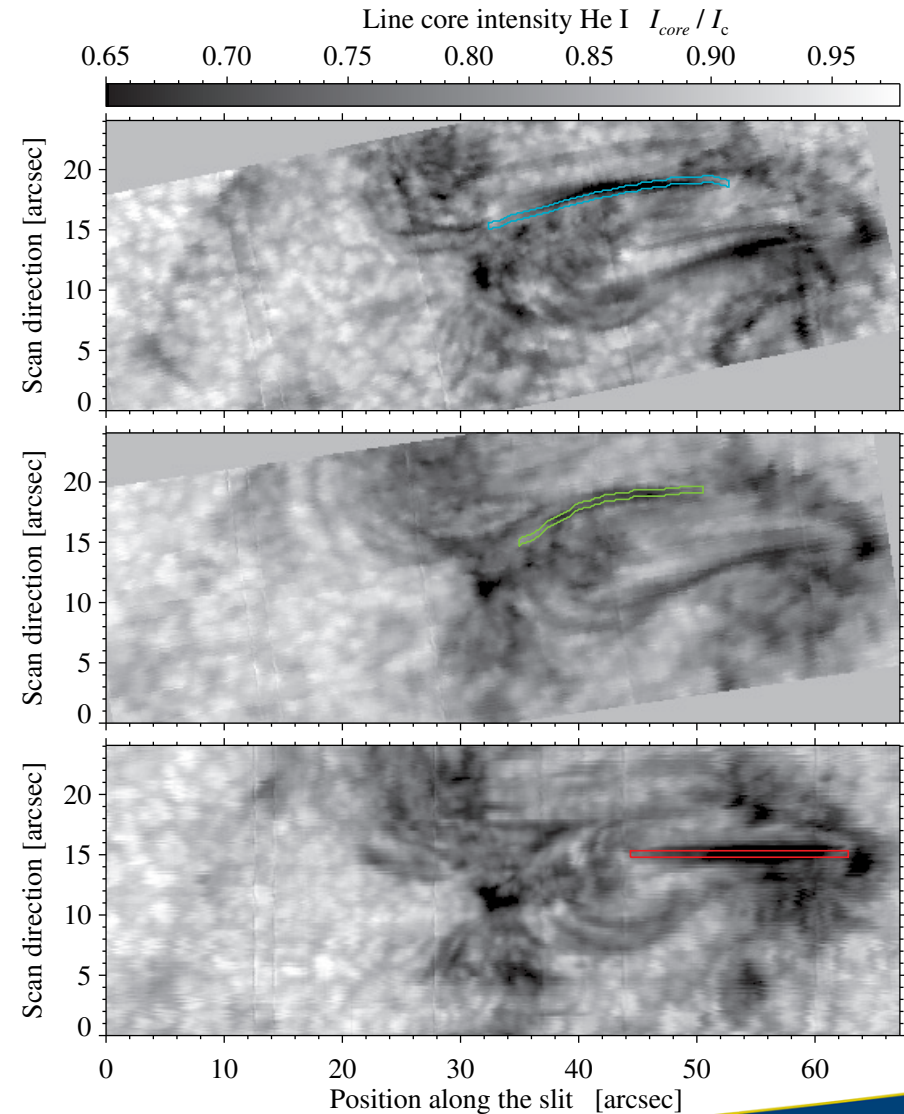
- ❑ Mean velocities of arch filaments
- ❑ Mean velocities of five pixels within a column
- ❑ Upflows at the loop-tops of the arch filaments
- ❑ Reaching chromospheric heights, the magnetic loops become visible in $H\alpha$, He I, and Ca II. Material gradually drains from the loops to the footpoints
- ❑ Supersonic downflows at the footpoints



Temporal evolution of an arch filament system

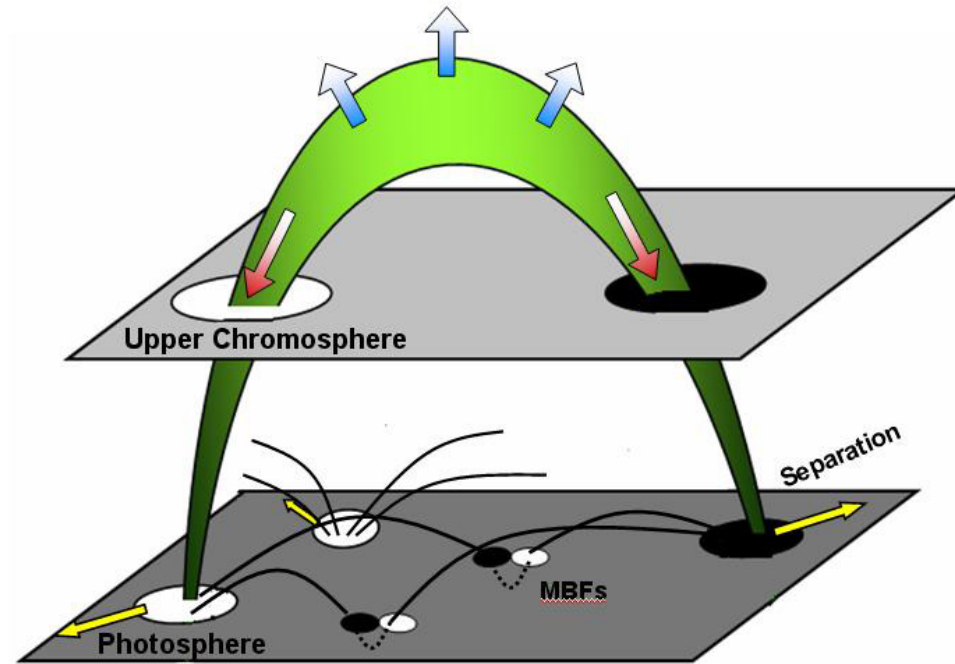
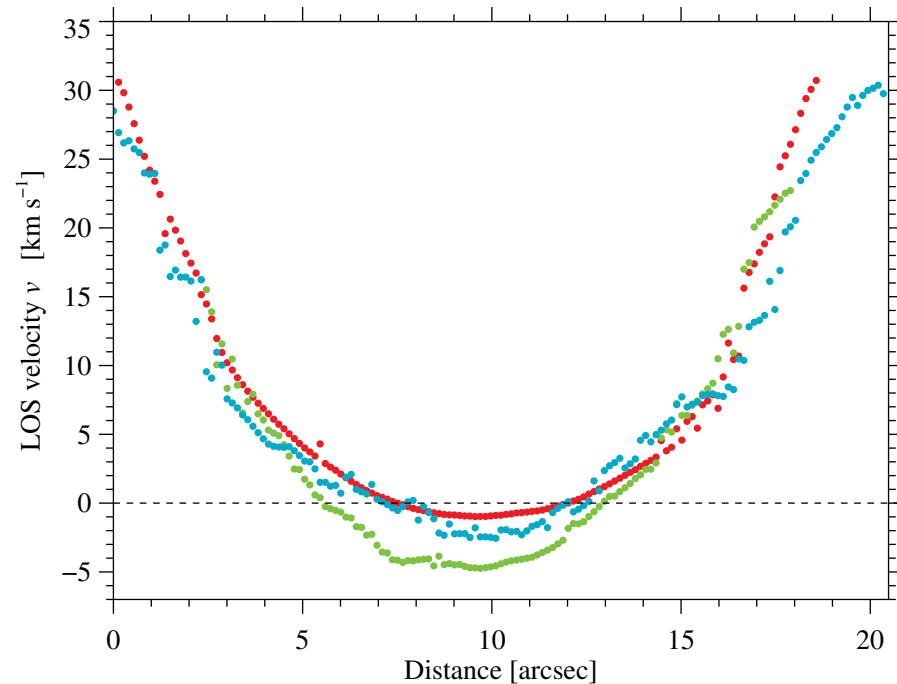


González Manrique et al. (2017, in preparation)



Temporal evolution of an arch filament system

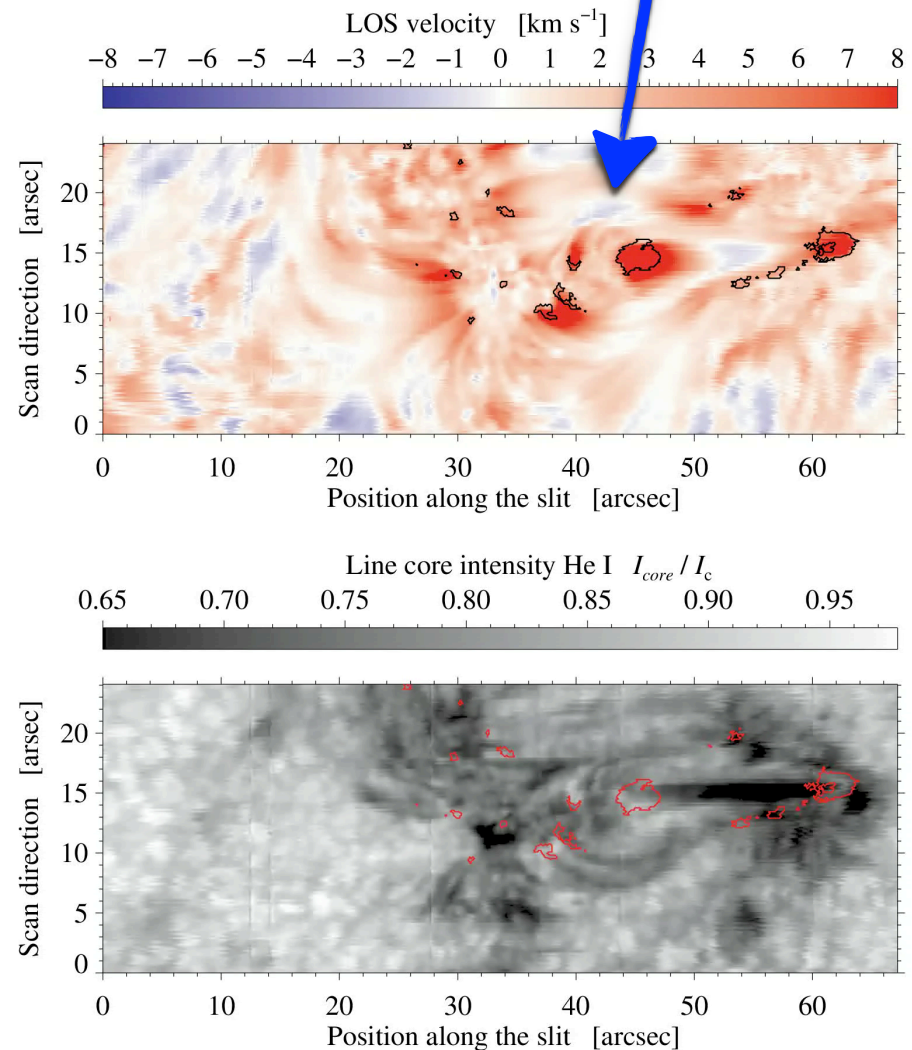
Xu, Lagg, and Solanki (2010)



- ❑ Upflows at the loop-tops of the arch filaments
- ❑ Reaching chromospheric heights, the magnetic loops become visible in $H\alpha$, He I, and Ca II. Material gradually drains from the loops to the footpoints
- ❑ Supersonic downflows at the footpoints

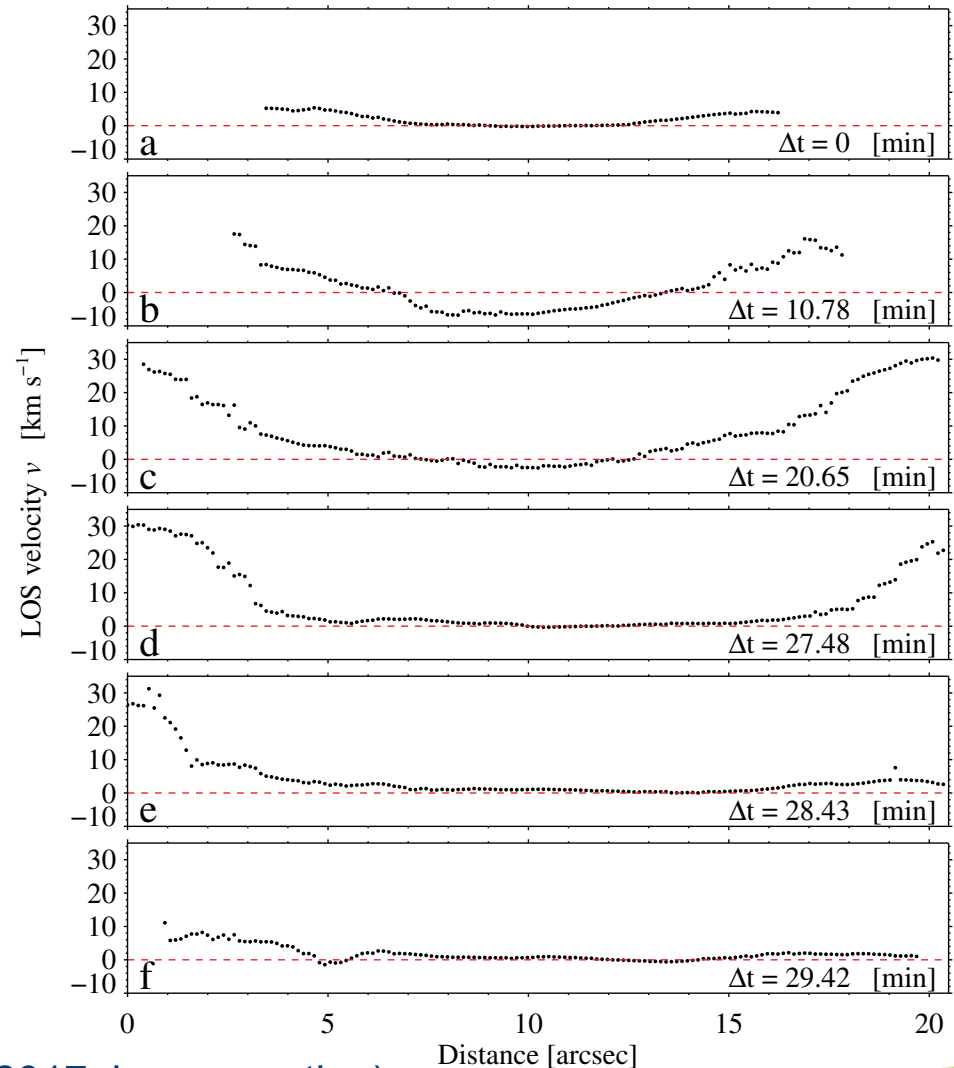
Temporal evolution of an arch filament system

- ❑ Temporal evolution of one arch filament
- ❑ Life-time of the arch filament is about 25-30 min
- ❑ Initially the velocities are near 0 km/s at the loop-tops and there are small downflows at the footpoints.
- ❑ With time the loop-tops present high upflows and supersonic downflows at the footpoints.
- ❑ The distance increase with time
- ❑ Near the end the velocities approach zero in the whole arch filament



Temporal evolution of an arch filament system

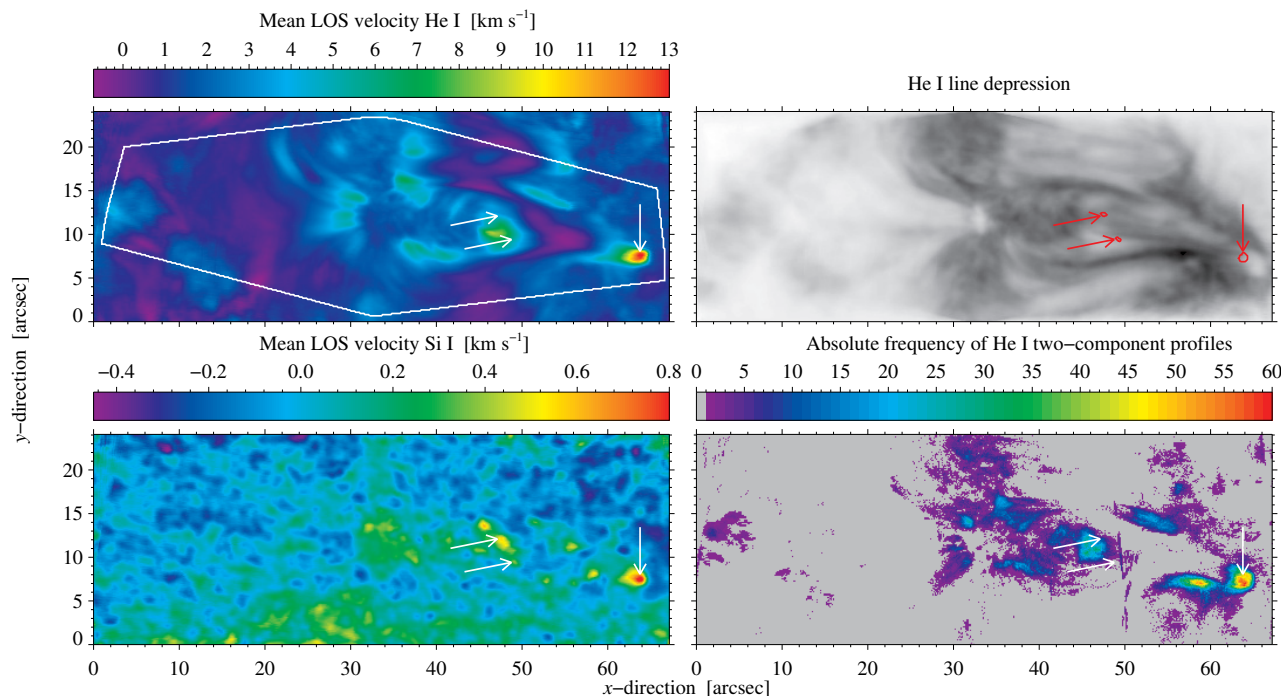
- Temporal evolution of one arch filament
- Life-time of the arch filament is about 25-30 min
- Initially the velocities are near 0 km/s at the loop-tops and there are small downflows at the footpoints.
- With time the loop-tops present high upflows and supersonic downflows at the footpoints.
- The distance increase with time
- Near the end the velocities approach zero in the whole arch filament



González Manrique et al. (2017, in preparation)

Tracking high-velocity features

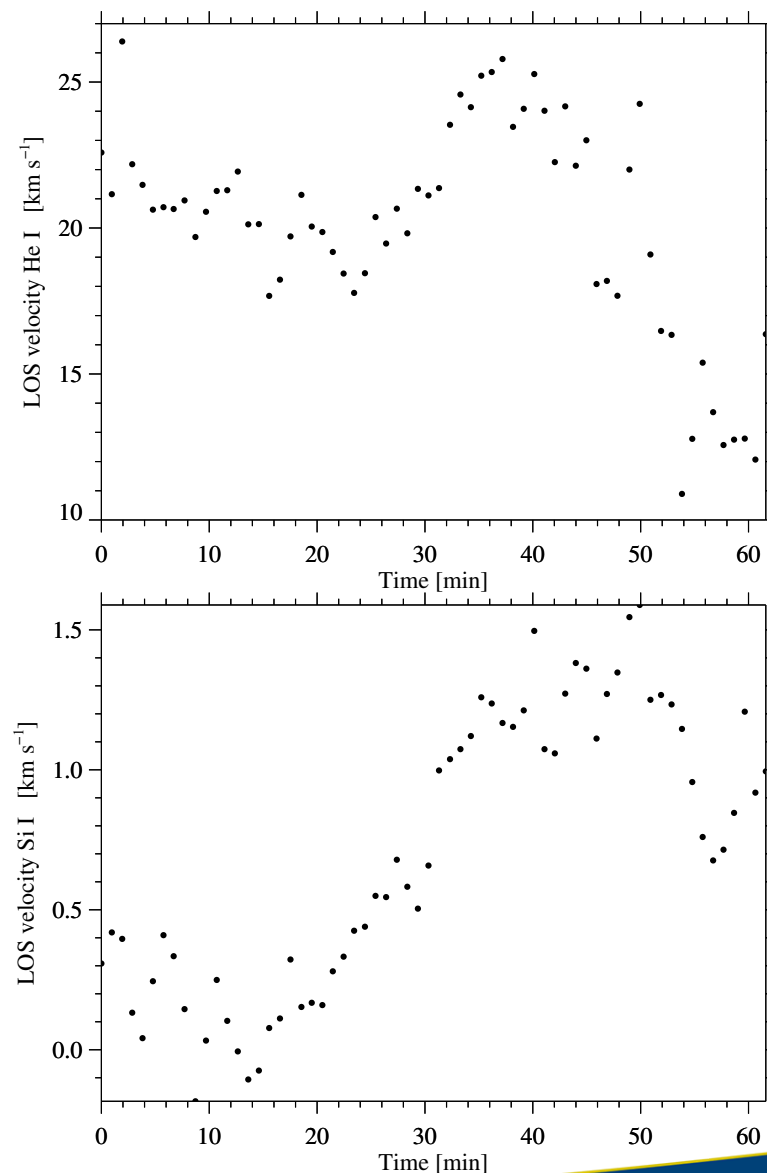
- Mean velocities for each pixel of 16 images of the common FOV
- 48 mean velocity maps
- 16 maps ~16 minutes
- Lifetime of granules ~5 minutes
- Contours represent mean velocities higher than $\bar{v} + 3\sigma$ for Si I
- Consistent mean velocities in the footpoint near the right pore



González Manrique et al. (2017, in preparation)

Tracking high-velocity features

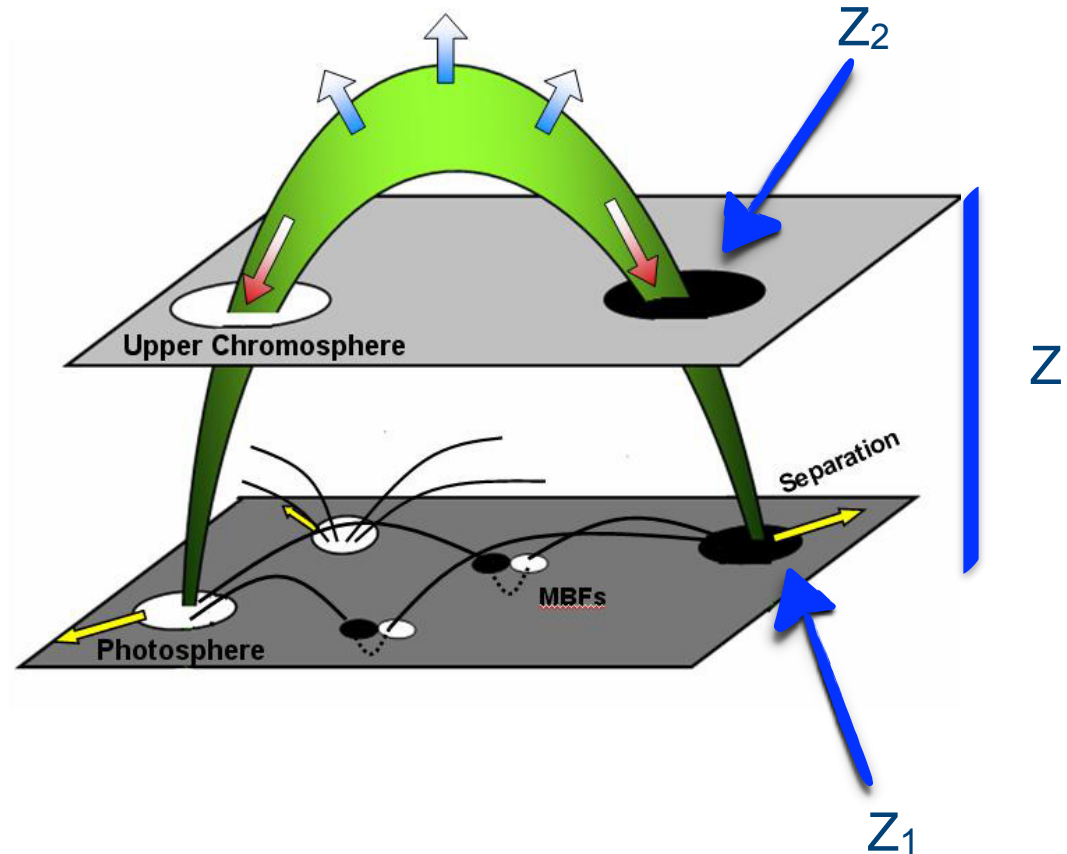
- ❑ Mean velocities for each pixel of 16 images of the common FOV
- ❑ 48 mean velocity maps
- ❑ 16 maps ~16 minutes
- ❑ Lifetime of granules ~15 minutes
- ❑ Contours represent mean velocities higher than $\bar{v} + 3\sigma$ for Si I
- ❑ Clear consistent mean velocities in the footpoint near the right pore for the Si I map



Tracking high-velocity features

Xu, Lagg, and Solanki (2010)

- ❑ The plasma moves from the chromosphere to the photosphere along a flux tube
- ❑ The area of the tube is decreasing with distance and the plasma is getting denser
- ❑ Assumption that magnetic flux is conserved



Tracking high-velocity features

Xu, Lagg, and Solanki (2010)

Stationary fluid:

$$\nabla(\rho v) = 0$$

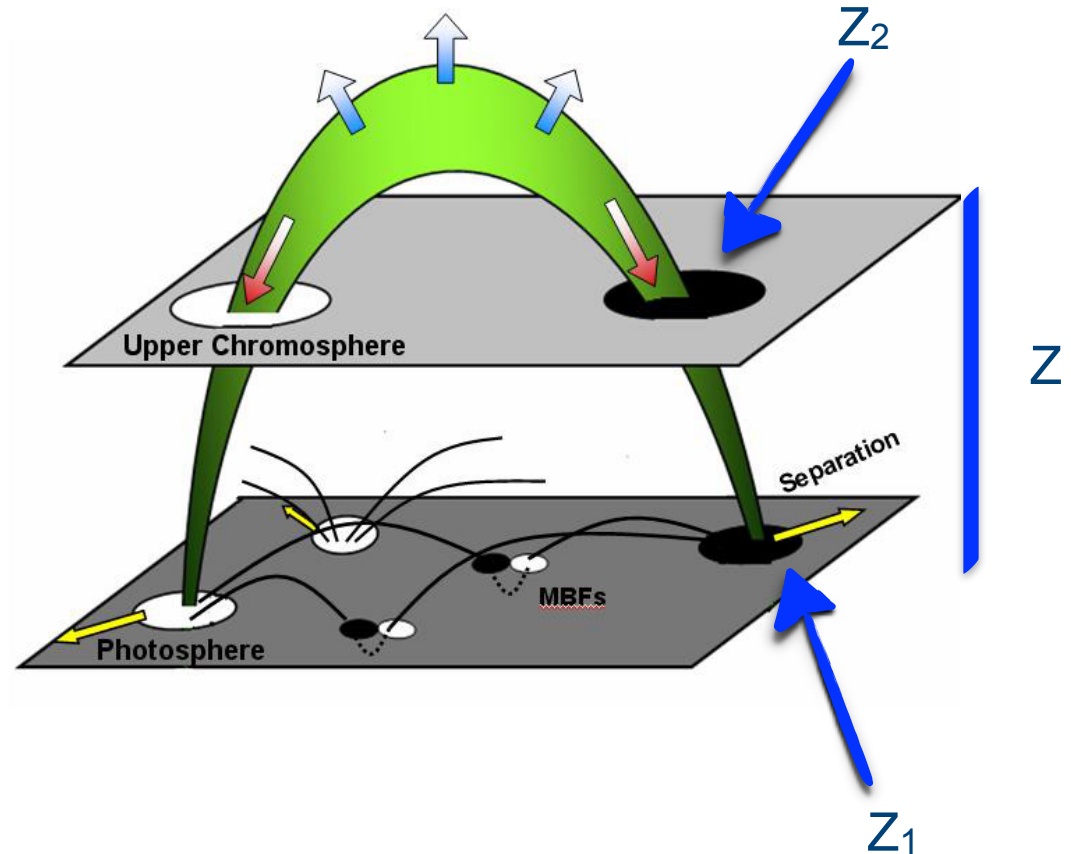
The fluid moves along the magnetic field lines:

$$\rho v S = cte$$

$$BS = cte$$

Conservation of magnetic flux:

$$\frac{\rho v}{B} = cte$$



Tracking high-velocity features

Xu, Lagg, and Solanki (2010)

Hydrostatic equilibrium:

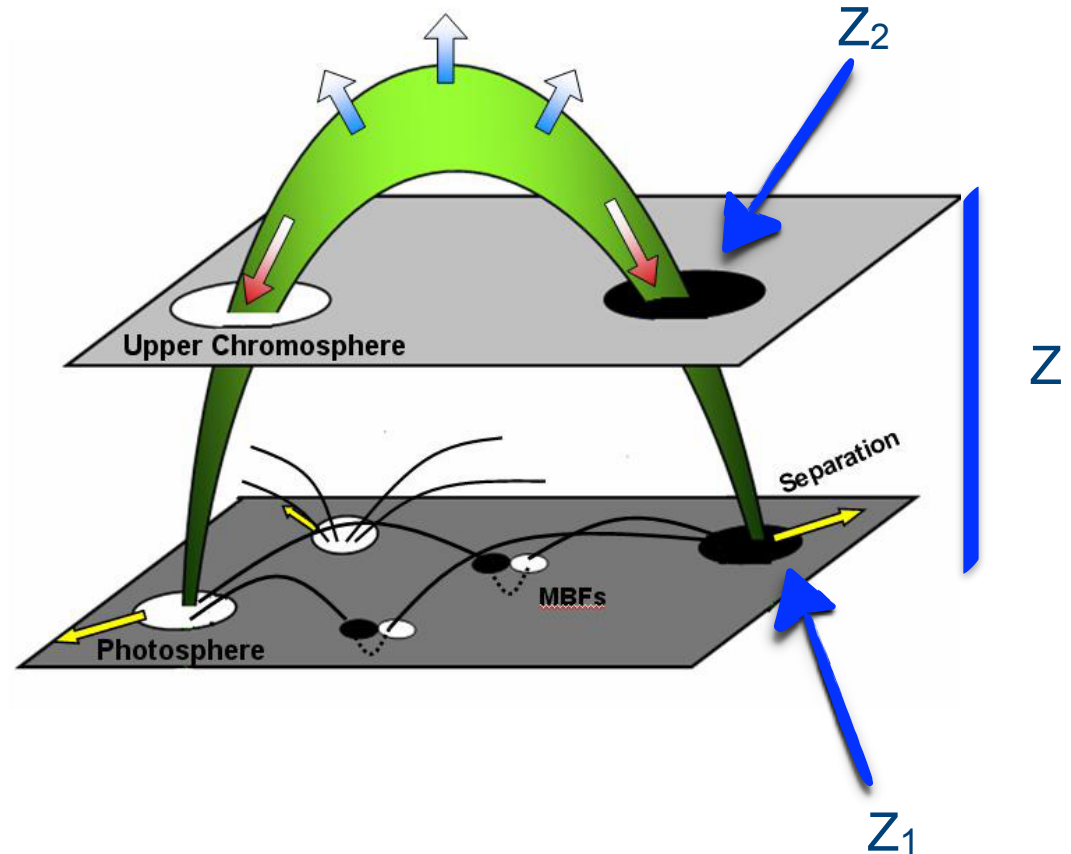
$$\rho \sim e^{(-z/H)}$$

Thin flux tube:

$$B \sim e^{(-z/2H)}$$

Isotherm atmosphere:

$$H = RT/\rho g$$



Tracking high-velocity features

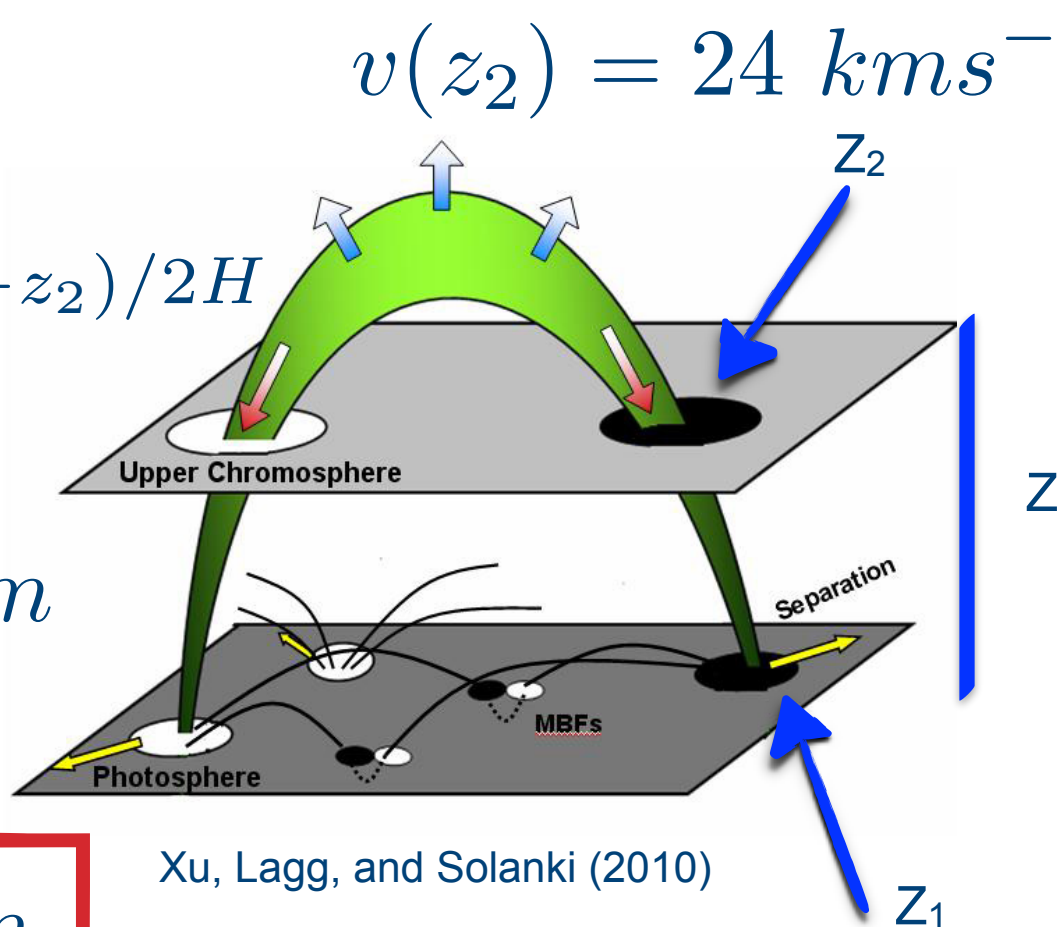
$$v(z) = e^{z/2H}$$

$$v(z_2) = 24 \text{ km s}^{-1}$$

$$v(z_1)/v(z_2) = e^{(z_1 - z_2)/2H}$$

$$H = 100 - 150 \text{ km}$$

$$Z \sim 600 - 900 \text{ km}$$



$$v(z_1) = 1.2 \text{ km s}^{-1}$$

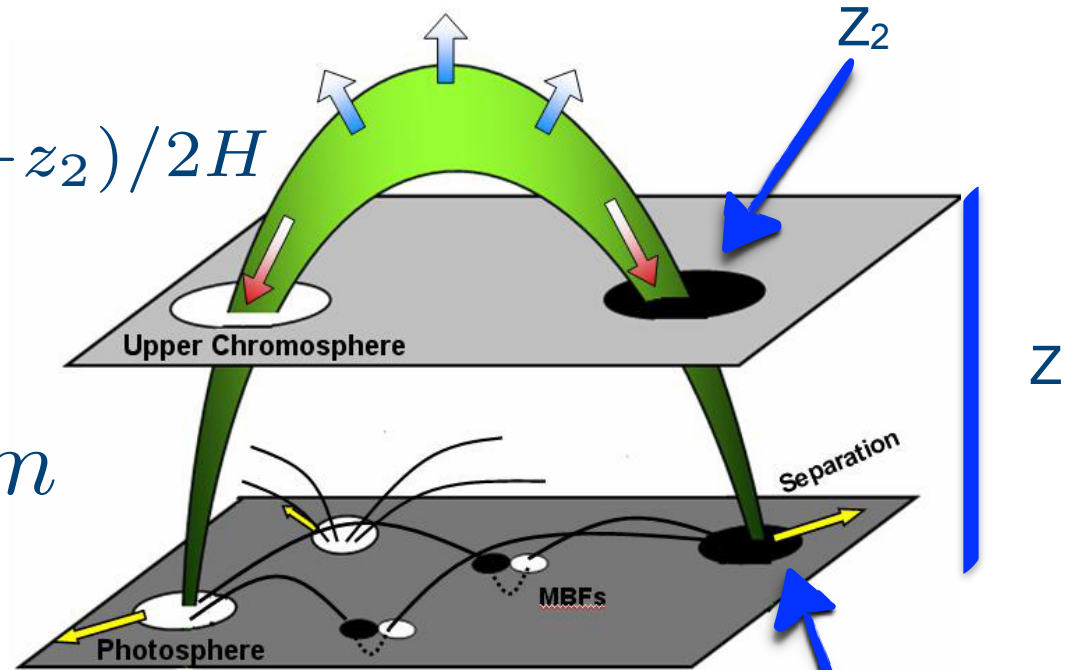
Tracking high-velocity features

$$v(z) = e^{z/2H}$$

$$v(z_2) = 24 \text{ km s}^{-1}$$

$$v(z_1)/v(z_2) = e^{(z_1 - z_2)/2H}$$

$$H = 100 - 150 \text{ km}$$



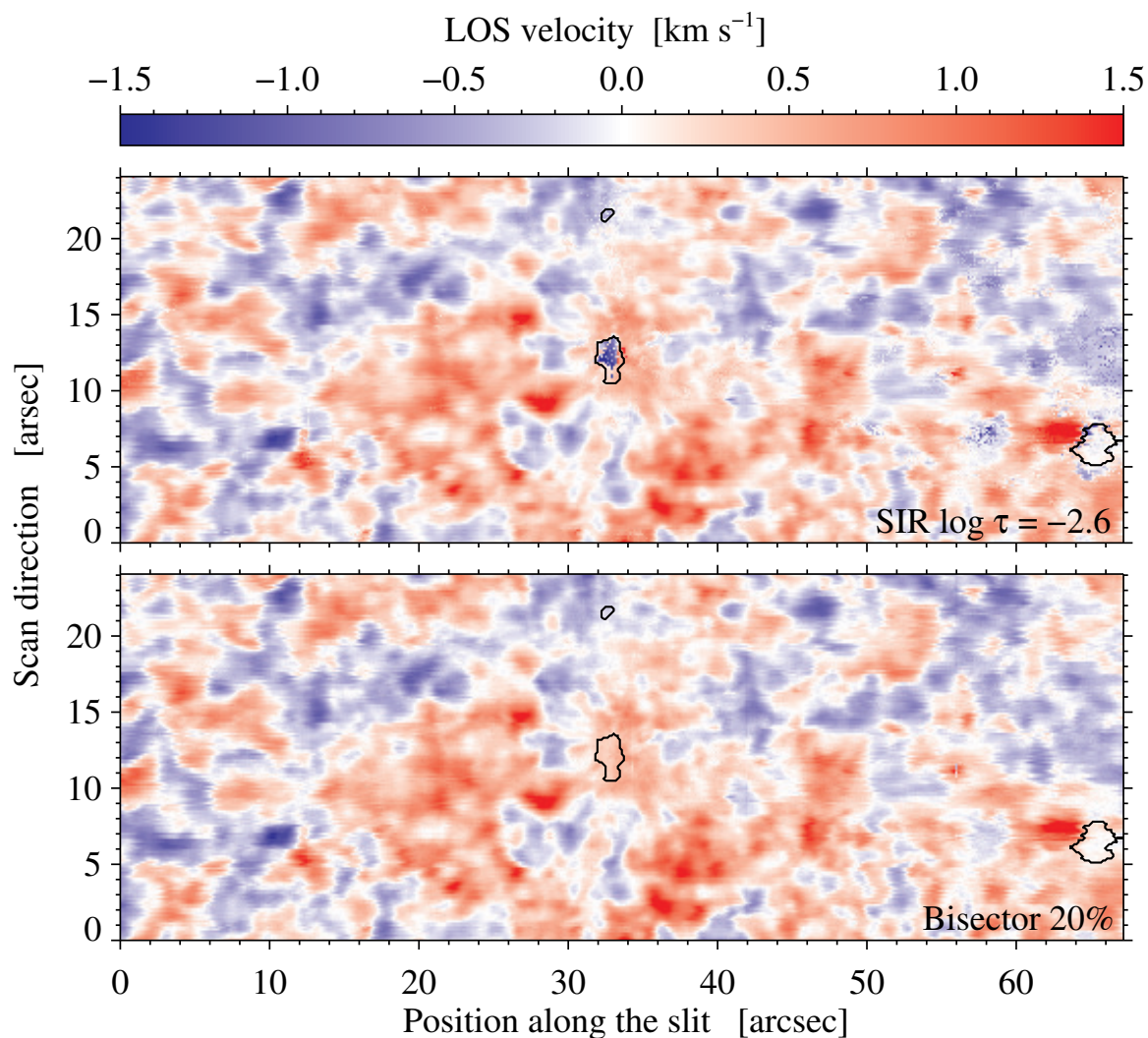
Xu, Lagg, and Solanki (2010)

$$Z \sim 1100 \text{ km}$$

$$v(z_1) = 0.7 \text{ km s}^{-1}$$

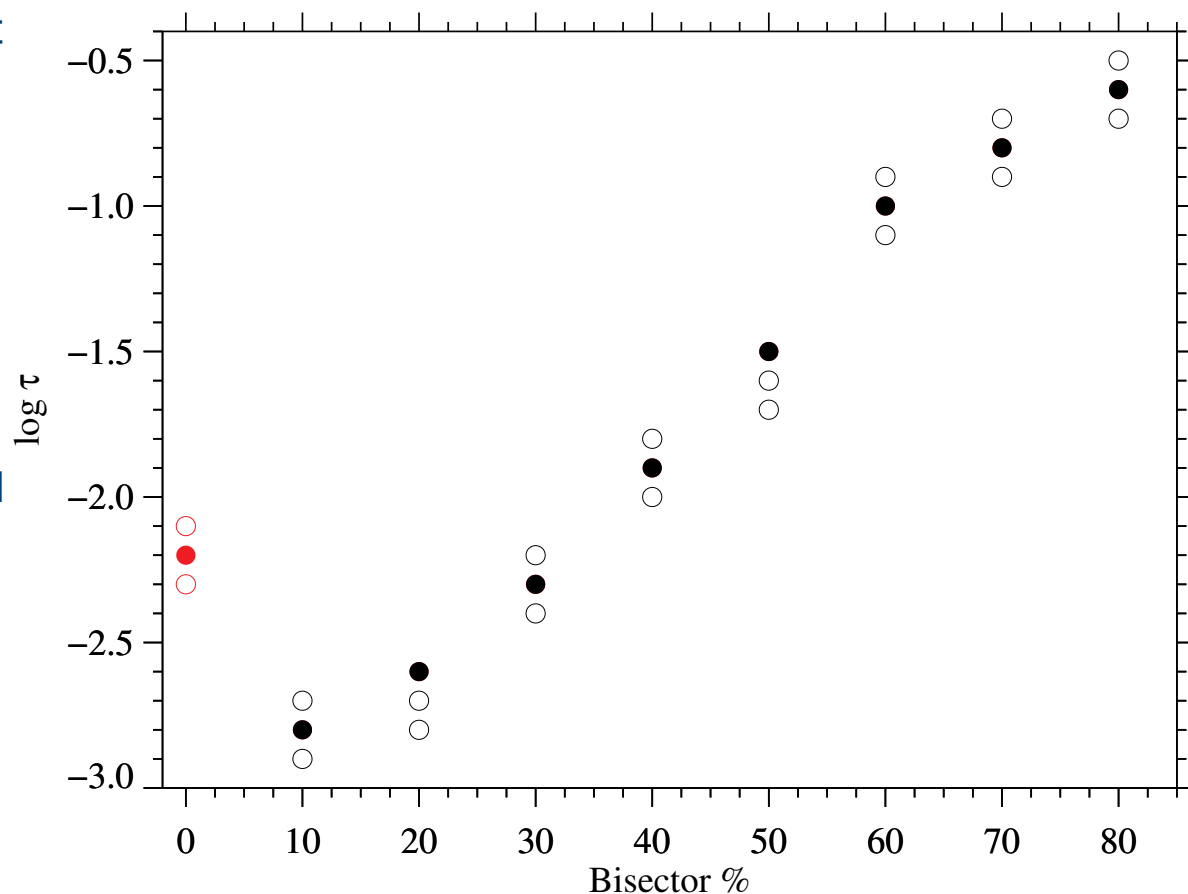
Si I SIR results vs. bisectors

- ❑ Velocity maps inferred from the Si I line using two different methods: SIR code (top) and bisectors (bottom)
- ❑ Highest correlation between both methods resulted in 97.8% and a $\log \tau = -2.6$ from SIR
- ❑ Contours correspond to dark areas in the continuum images. Correlation computed excluding the dark areas.
- ❑ Height-dependent bisectors method and SIR results
- ❑ The three bullets represent the three highest correlation between both methods.
- ❑ The red bullets refer to the velocity in the line core.



Si I SIR results vs. bisectors

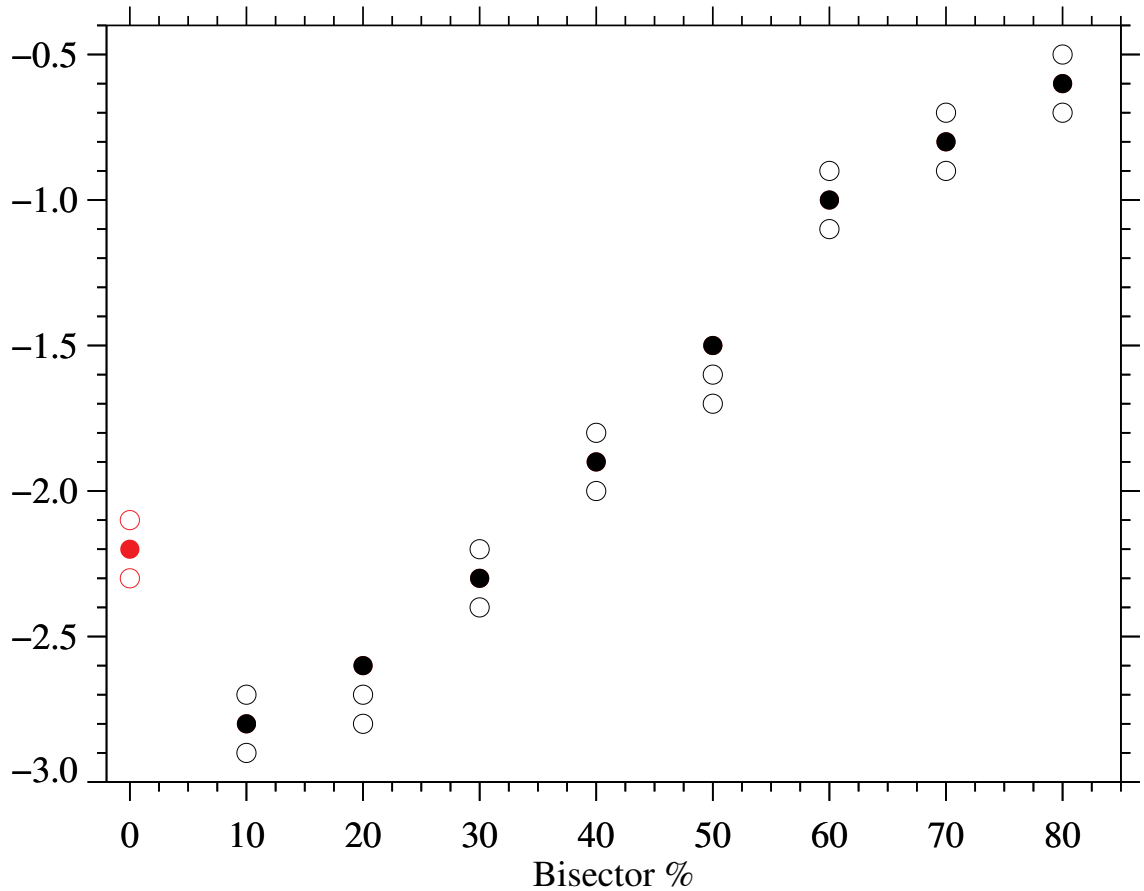
- Velocity maps inferred from the Si I line using two different methods: SIR code (top) and bisectors (bottom)
- Highest correlation between both methods resulted in 97.8% and a $\log \tau = -2.6$ from SIR
- Contours correspond to dark areas in the continuum images. Correlation computed excluding the dark areas.
- Height-Dependent bisectors method and SIR results
- The three bullets represent the three highest correlation between both methods.
- The red bullets refer to the velocity in the line core.



González Manrique et al. (2017, in preparation)

Si I SIR results vs. bisectors

<i>Bisector [%]</i>	<i>Correlation [%]</i>	<i>log τ</i>
10	97.2	-2.8
20	97.8	-2.6
30	97.8	-2.3
40	97.2	-1.9
50	96.7	-1.5
60	97.0	-1.0
70	96.9	-0.8
80	95.1	-0.6



Conclusions and Outlook

- We used a simple and fast technique for determining the velocity of multiple atmospheric components within a single spatial pixel. Good fits and reasonable velocity values.
- With the available data we are able to follow during one hour the dynamics and temporal evolution of chromospheric and photospheric structures.
- We can confirm the lifetime of arch filaments presented in other studies. We presented the evolution of the He I velocities within a single arch filament. We confirm supersonic LOS velocities at the footpoints.
- We studied the link between the chromospheric filamentary structures and the underlying photosphere structures. We demonstrated that the plasma of the chromospheric structures, which exhibit permanent supersonic downflows near the footpoints reach the photosphere. We can estimate an approximate distance between the chromospheric footpoints observed with the He I line and the photospheric footpoints observed with the Si I line.
- We studied the height-dependence between the bisectors method and SIR results
- NICOLE inversions at a footpoint with the Ca II NIR line at 854.2 nm and study the chromospheric velocities.



Thank you!

Method

- ❑ Most of the He I intensity profiles show the expected two spectral lines.
- ❑ Around 3% show a clear signature of a fast component
- ❑ Assume all the profiles have only the slow component
- ❑ We use single Lorentzian profile to fit the He I profiles
- ❑ Equation set to unity to normalize the synthetic intensity continuum
- ❑ Levenberg-Marquardt least-squares minimization
- ❑ Upper and lower bounding limit
- ❑ Spectral range depending of the amplitude
- ❑ Zero reference 10830.30 Å

Single-Lorentzian

$$F = 1 - \frac{A_0}{u^2 + 1}$$

$$u = \frac{x - A_1}{A_2}$$

A_0 = Amplitude

A_1 = Peak centroid

A_2 = Half-width-at-half-minimum

Method

- ❑ Fitting all profiles double-Lorentzian profile
- ❑ Two different wavelengths ranges depending of the position of the line core
- ❑ Below 10830.49 Å the range is [-0.83, +1.73] Å respect to the line core
- ❑ Above 10830.49 Å the range is [-1.37, +1.73] Å respect to the line core
- ❑ Initial estimates of the fit parameters A_0 - A_5 were based on the single-Lorentzian fits
- ❑ To localize the dual-flow profiles different types of these profiles were selected and correlated with all the profiles of the map.
- ❑ Threshold 98% of the mean of the correlation

double-Lorentzian

$$F = 1 - \frac{A_0}{u_1^2 + 1} - \frac{A_3}{u_2^2 + 1}$$

$$u_1 = \frac{x - A_1}{A_2}$$

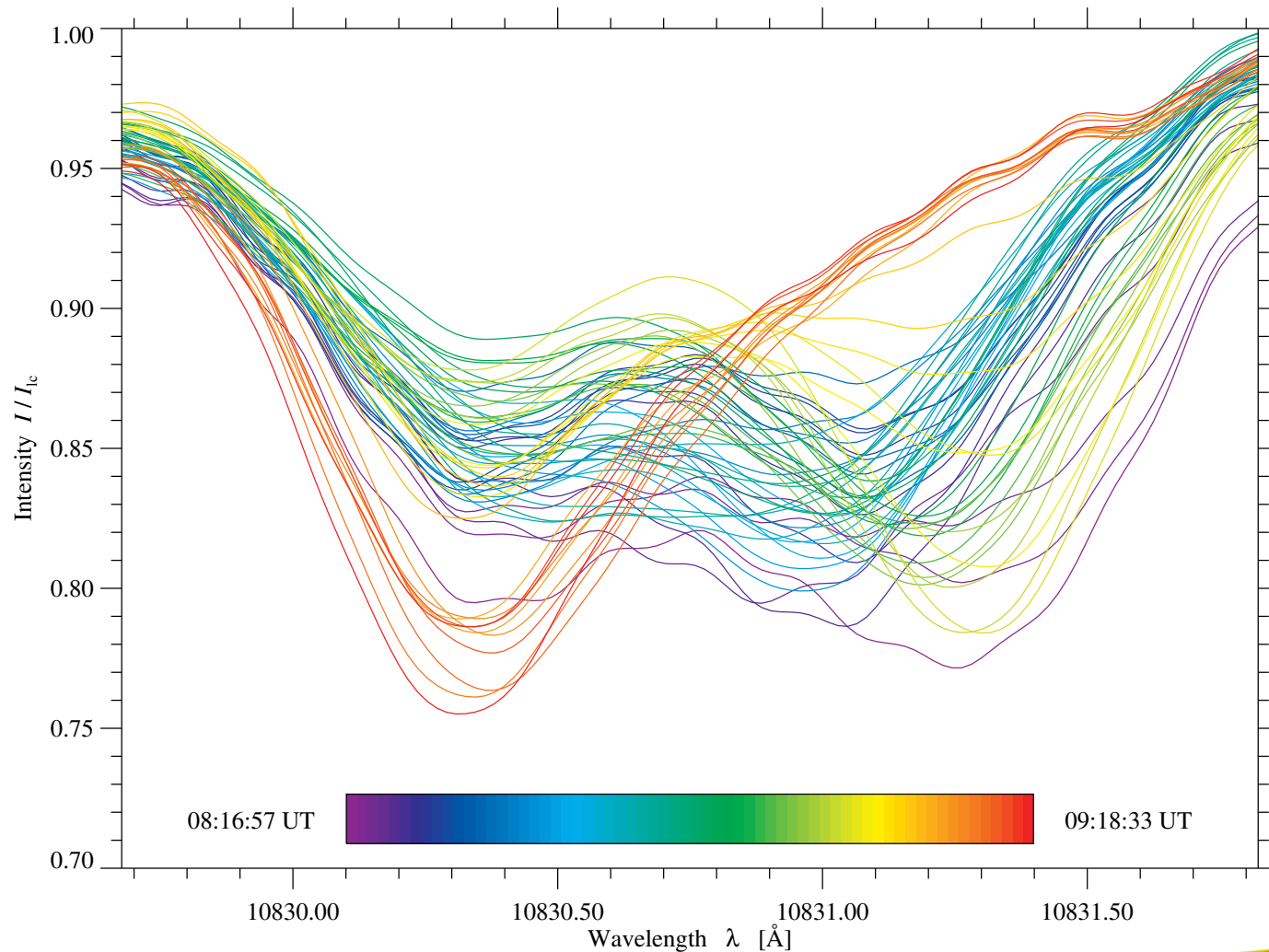
$$u_2 = \frac{x - A_4}{A_5}$$

$A_{0,3}$ = Amplitude

$A_{1,4}$ = Peak centroid

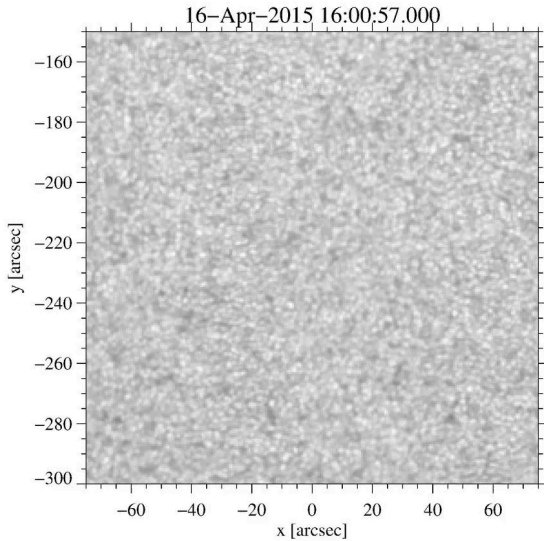
$A_{2,5}$ = Half-width-at-half-minimum

Temporal evolution of spectral profiles

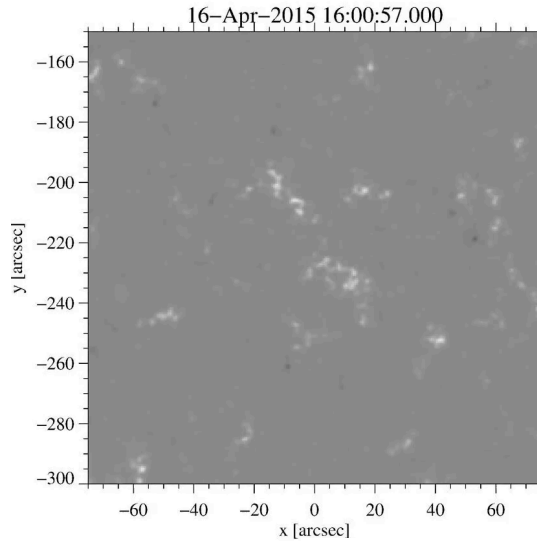


Complement data with SDO (HMI, AIA)

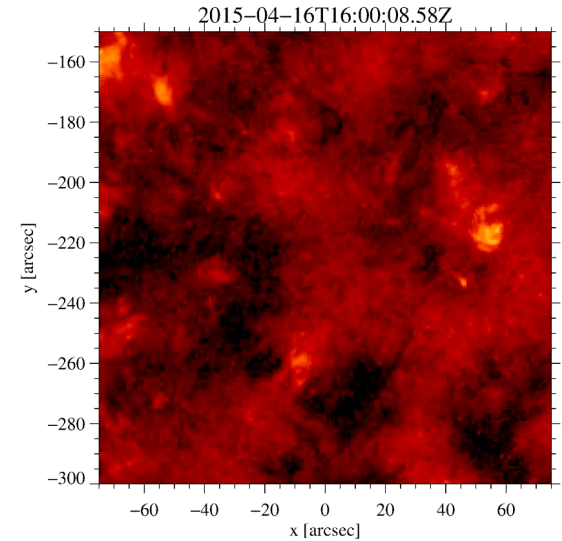
HMI: Continuum



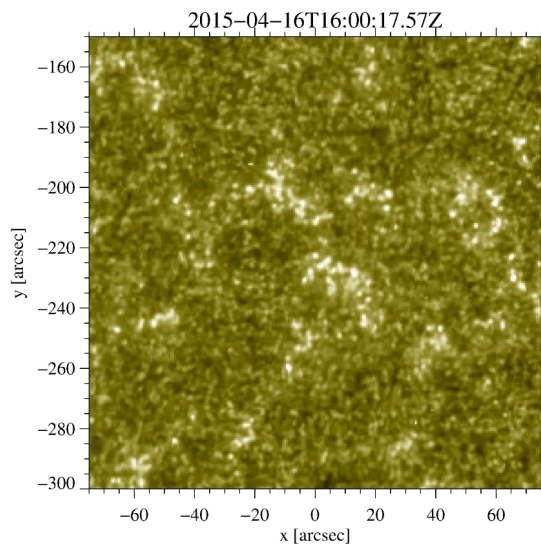
HMI: Magnetograms



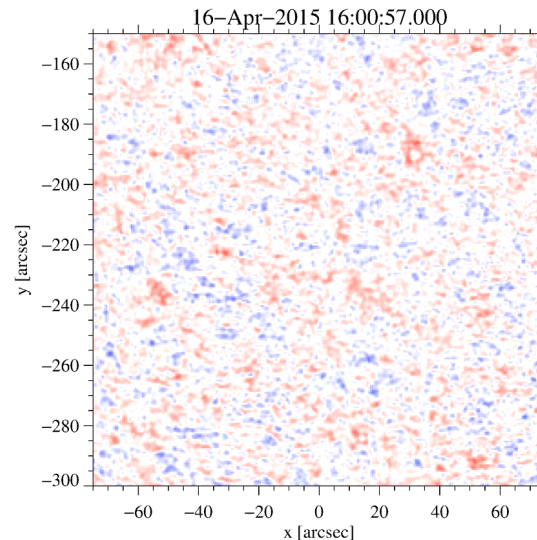
AIA: 304 Å



AIA: 1600 Å Continuum

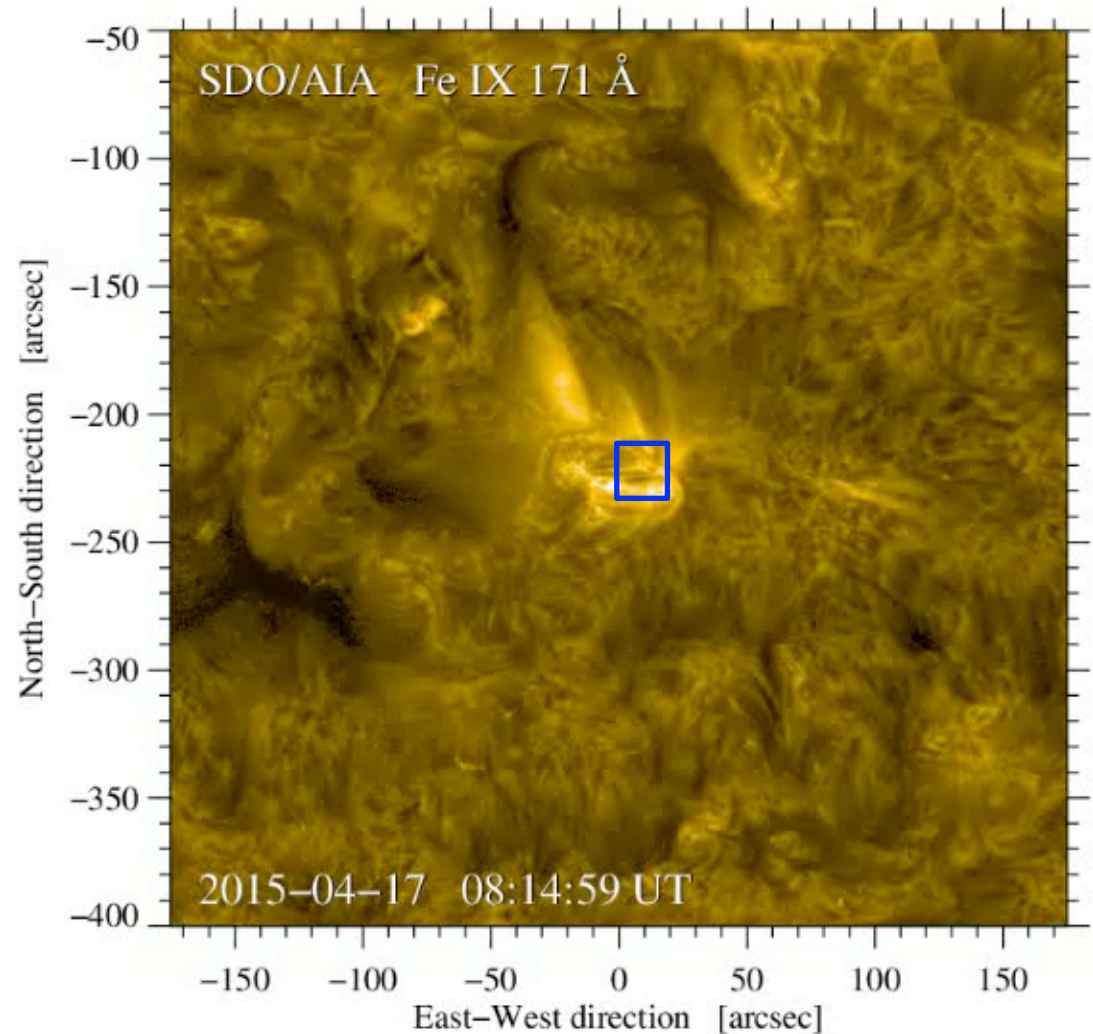


HMI: LOS Velocity



Complement data with SDO (HMI, AIA)

- ❑ Start:
17 April 2015 8:15 UT
- ❑ Finish: 17 April 2015
9:20 UT
- ❑ Same time range as
observations
- ❑ Image enhancement
using NAFE
- ❑ AIA: 171 Å
- ❑ Microflare at the end of
the movie?



SIR inversions CRISP 617.3 nm

